Stem Cell Research & Therapy

RESEARCH

Open Access

Prolonged cultivation enhances the stimulatory activity of hiPSC mesenchymal progenitor-derived conditioned medium

Darja Marolt Presen[1,2*], Vanessa Goeschl[1,2], Dominik Hanetseder[1,2], Laura Ogrin[1,2], Alexandra-Larissa Stetco[1,2], Anja Tansek[1,2], Laura Pozenel[1,2], Bella Bruszel[3], Goran Mitulovic[4,5], Johannes Oesterreicher[1,2], Johannes Zipperle[1,2], Barbara Schaedl[1,2,6], Wolfgang Holnthoner[1,2], Johannes Grillari[1,2,7] and Heinz Redl[1,2]

Abstract

Background Human induced pluripotent stem cells represent a scalable source of youthful tissue progenitors and secretomes for regenerative therapies. The aim of our study was to investigate the potential of conditioned medium (CM) from hiPSC-mesenchymal progenitors (hiPSC-MPs) to stimulate osteogenic differentiation of human bone marrow-derived mesenchymal stromal cells (MSCs). We also investigated whether prolonged cultivation or osteogenic pre-differentiation of hiPSC-MPs could enhance the stimulatory activity of CM.

Methods MSCs were isolated from 13 donors (age 20–90 years). CM derived from hiPSC-MPs was added to the MSC cultures and the effects on proliferation and osteogenic differentiation were examined after 14 days and 6 weeks. The stimulatory activity of hiPSC-MP-CM was compared with the activity of MSC-derived CM and with the activity of CM prepared from hiPSC-MPs pre-cultured in growth or osteogenic medium for 14 days. Comparative proteomic analysis of CM was performed to gain insight into the molecular components responsible for the stimulatory activity.

Results Primary bone marrow-derived MSC exhibited variability, with a tendency towards lower proliferation and tri-lineage differentiation in older donors. hiPSC-MP-CM increased the proliferation and alkaline phosphatase activity of MSC from several adult/aged donors after 14 days of continuous supplementation under osteogenic conditions. However, CM supplementation failed to improve the mineralization of MSC pellets after 6 weeks under osteogenic conditions. hiPSC-MP-CM showed greater enhancement of proliferation and ALP activity than CM derived from bone marrow-derived MSCs. Moreover, 14-day cultivation but not osteogenic pre-differentiation of hiPSC-MPs strongly enhanced CM stimulatory activity. Quantitative proteomic analysis of d14-CM revealed a distinct profile of components that formed a highly interconnected associations network with two clusters, one functionally associated with binding and organization of actin/cytoskeletal components and the other with structural constituents of the extracellular matrix, collagen, and growth factor binding. Several hub proteins were identified that were reported to have functions in cell-extracellular matrix interaction, osteogenic differentiation and development.

*Correspondence:
Darja Marolt Presen
darja.marolt.presen@ki.si

Full list of author information is available at the end of the article

Conclusions Our data show that hiPSC-MP-CM enhances early osteogenic differentiation of human bone marrow-derived MSCs and that prolonged cultivation of hiPSC-MPs enhances CM-stimulatory activity. Proteomic analysis of the upregulated protein components provides the basis for further optimization of hiPSC-MP-CM for bone regenerative therapies.

Graphical Abstract

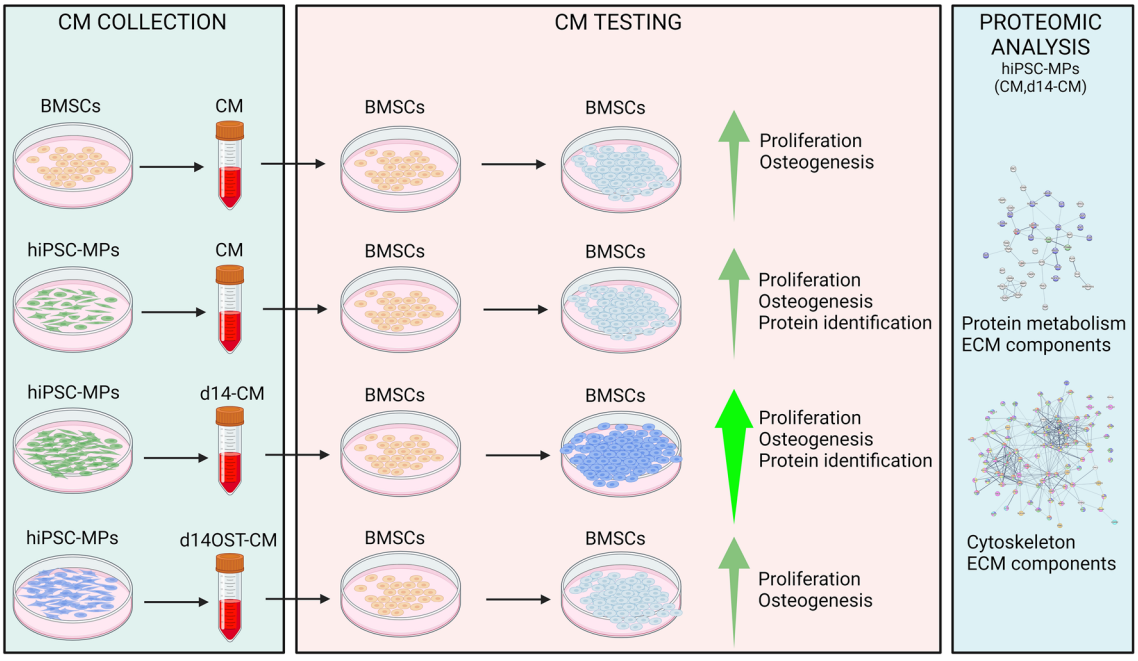

Keywords Conditioned medium, Secretome, Human iPSCs, Human bone marrow mesenchymal stromal cells, Mesenchymal progenitors, Osteogenic differentiation, Proteomic analysis, Aging

Background

Mesenchymal stromal cells (MSCs) exhibit excellent osteogenic differentiation potential and have been extensively studied for cell therapies, bone tissue engineering and regenerative therapies [1]. Despite numerous in vitro studies demonstrating the differentiation of MSCs and the formation of new bone-like matrix, in vivo studies have shown that the survival and engraftment of MSCs after transplantation into experimental bone defects is low, indicating the regenerative effects of MSC secretome [2–4].

The MSC secretome, often obtained from MSC cultures as conditioned medium (CM), contains a complex mixture of secreted soluble signals and extracellular vesicles (EVs) that have been shown to promote stem and progenitor cell migration, proliferation and differentiation [5, 6]. For therapeutic applications, CM offers important advantages over viable cell therapies, including the possibility of product sterilization and less stringent handling and storage requirements [7]. Unfractionated CM from primary human MSCs has already been shown to stimulate osteogenic differentiation and improve regeneration of bone defects in rodent models. In particular, human bone marrow-derived MSC-CM has been shown to promote healing of critical-sized calvarial bone defects in rats to a greater extent than the transplanted viable MSCs [8]. In a mouse model of distraction osteogenesis, local administration of bone marrow-derived MSC-CM accelerated the formation of new callus and bone healing through the recruitment of bone marrow-derived MSCs, endothelial cells and/or endothelial progenitor cells and the formation of a neo-angiogenic network [9]. Similarly, CM showed a therapeutic effect in a bisphosphonate-induced osteonecrosis-like model in rats [10]. The soluble CM components involved in these bone regenerative effects included vascular endothelial growth factor (VEGF), insulin-like growth factor-1 (IGF-1), transforming growth factor-β1 (TGF-β1) and monocyte chemoattractant protein-1 (MCP-1) [11–13]. In addition, the vesicular fraction of CM was shown to enhance fracture healing in a mouse model [14], and might present several advantages for clinical translation (as reviewed in [1]). EVs secreted by rat or human MSCs from bone marrow, adipose tissue, gum tissue, umbilical

cord and human induced pluripotent stem cells (hiPSCs) have been shown to enhance osteogenic differentiation in vitro [15–22] and promote bone healing in rodent models [15, 18–23]. Molecular signals attributed to MSC-EVs include Wnt-3a [16], miR-196a [21], HIF-1α/VEGF [23], PI3K/Akt [20] and BMP-2/Smad1/RUNX2 signaling pathways [22].

In previous studies, primary MSCs from young donors and young adult animal models were frequently used to prepare and test the effects of CM on osteogenic differentiation. However, advanced patient age is one of the main risk factors for delayed or failed bone healing [24, 25]. With advanced age, changes in the systemic environment [26, 27] and bone tissue [28] can negatively impact the number and regenerative potential of MSCs [29]. In addition, the aging of MSCs, the inherent variability of MSCs derived from different donors, and the limited cell quantities and/or regenerative potential pose significant challenges for the clinical implementation of treatments using CM from primary human MSCs.

In contrast, human induced pluripotent stem cells (hiPSCs) represent a virtually unlimited source of youthful, embryonic-like mesenchymal tissue progenitors (hiPSC-MPs), that have a high proliferation and differentiation potential [30, 31]. Therefore, hiPSC-MPs can be standardized and upscaled for CM production. The original aim of our study was to investigate whether hiPSC-MP-derived CM can enhance osteogenic differentiation of human bone marrow-derived MSCs isolated from donors of different ages. In previous studies on the effect of CM on osteogenic differentiation and bone formation, CM was mostly prepared from subconfluent MSC cultures [8–10, 32]. We aimed to determine whether prolonged cultivation or pre-differentiation of hiPSC-MS under osteogenic conditions could enhance the stimulatory activity of CM. Finally, we performed quantitative proteomic analysis to identify molecular signaling components associated with the enhanced stimulatory activity of d14-CM from prolonged hiPSC-MPs cultures.

Methods

Materials

Ascorbic acid-2-phosphate, ß-glycerophosphate, calf thymus DNA standard, dexamethasone, Dulbecco's Modified Eagle's Medium - high glucose (DMEM-hg), Dulbecco's phosphate buffered saline (DPBS), gelatin, fetal bovine serum (FBS), 3-isobutyl-1-methylxanthine (IBMX), L-glutamine solution (L-glut), L-proline, phosphate buffered saline (PBS), penicillin-streptomycin (pen-strep), p-nitrophenol standard, trypsin-EDTA (10 x solution), tissue culture water, transforming growth factor-beta 3 human (TGF-β3) and TRI Reagent® were purchased from Sigma-Aldrich (St.Louis, USA). DNase I, GlutaMAX, HyClone™ fetal bovine serum (HyClone-FBS), insulin-transferrin-selenium-ethanolamine supplement mixture (ITS-X), KnockOut™ DMEM (KO-DMEM), β-mercaptoethanol, nonessential amino-acids and sodium pyruvate were purchased from Thermo Fisher Scientific (Waltham, USA). Basic fibroblast growth factor (bFGF) was purchased from PreproTech (Rocky Hill, USA) or Thermo Fisher Scientific.

Isolation and cultivation of human bone marrow-derived MSCs

Human bone marrow MSCs were isolated from the femoral bone marrow of 11 patients (6 women, 5 men, aged 43 to 90 years) undergoing hip replacement surgery at the Lorenz Bohler Unfallkrankenhaus, Vienna, Austria, with informed consent and full ethical approval (Ethics Committee for the AUVA Hospitals No. 1/2005, February 9th 2006). In addition, mononuclear cells from the bone marrow of two young adult donors (20-year-old woman and 22-year-old man) were acquired from Lonza (Basel, Switzerland). An overview of the characteristics of the donors is shown in Fig. 1. For the isolation of MSCs, remnants of the femoral tissue were transferred to a Petri dish, minced and washed with DMEM-hg supplemented with 1% pen-strep to obtain the bone marrow. The harvested bone marrow was centrifuged at 300 x g for 5 min. Commercial bone marrow-derived mononuclear cells were thawed by dilution in pre-warmed DMEM-hg supplemented with 10% FBS and 1% pen-strep, and centrifuged at 300 x g for 5 min. The resulting cell pellets from both sources were resuspended and cultured in MSC growth medium consisting of DMEM-hg supplemented with 10% FBS, 1% pen-strep, 2 mM L-glutamine and 1 ng/ml bFGF to establish primary cultures. The cultures were incubated at 37 °C and 5% CO_2 with media changes twice a week. After reaching confluence, the plastic-adherent cells (i.e. MSCs) were trypsinized and subcultured at a seeding density of 5000 cells/cm^2. The potential for proliferation in vitro was assessed over 6 consecutive passages. At the end of each passage, cells were counted and cumulative cell growth was determined as previously reported [33], taking into account the cells used for the characterization analyses. Average specific proliferation rate was determined for passages 1–6 for the analysis of correlation with donor age.

Characterization of human bone marrow-derived MSCs

The profile of surface antigen expression was determined in passage 5 cells. Briefly, the cells were trypsinized, washed and resuspended in a blocking buffer (PBS with 1% FBS). Aliquots of 100,000 cells were incubated for 30 min on ice in the dark with fluorescence-conjugated primary antibodies against CD44 (Cat. No. 555478), CD73 (Cat. No. 550257), CD90 (Cat. No. 555596), CD146 (Cat. No. 561013), CD31 (Cat. No. 555446) and

A

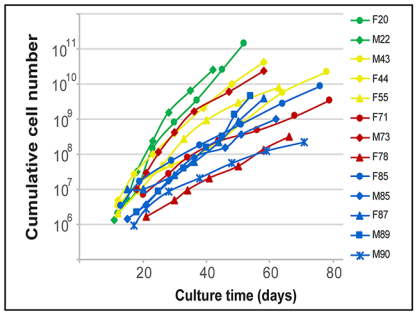

B

Donor		Osteogenesis	Chondrogenesis	Adipogenesis	Senescence
Age	Gender	Alizarin Red	Collagen Type II	Oil Red O	-gal. (% positive)
20	F	+++	+++	+++	2,8
22	M	+++	-	+++	0,4
43	M	-	+	+++	11,7
44	F	-	++	+	4,0
55	F	-	++	+	4,6
71	F	-	+	+	21,3
73	M	+	-	++	2,7
78	F	-	-	+	34,2
85	F	+	++	+	14,1
85	M	-	+	+	8,8
87	F	-	++	+	8,5
89	M	-	++	+	5,8
90	M	-	-	+	39,3

C

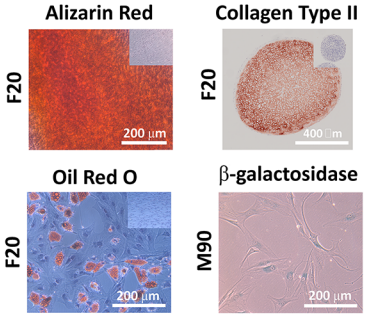

D

Donor		Surface antigen expression									
Age	Gender	CD44	CD73	CD90	CD105	CD146	CD14	CD31	CD34	CD45	HLA-DR
20	F	99,7	99,8	99,8	99,8	16,5	0,16	0,24	0,01	0,04	15,8
22	M	99,6	99,7	99,9	99,8	75,4	0,07	0,16	0,05	0,02	11,6
43	M	99,5	99,7	99,8	99,6	3,14	3,14	0,12	0,04	0,06	0,30
44	F	98,3	98,3	98,9	98,4	38,7	0,31	0,08	0,08	0,06	2,92
55	F	99,8	99,8	99,9	99,8	1,92	1,46	0,11	0,01	0,01	6,03
71	F	99,6	99,4	99,6	99,4	24,6	4,36	0,17	0,13	0,10	17,8
73	M	99,9	99,8	99,9	99,7	69,7	0,07	0,50	0,02	0,02	61,2
78	F	99,5	99,9	99,9	99,8	1,67	2,48	0,02	0,07	0,04	0,15
85	F	99,3	99,4	99,5	99,0	1,66	0,26	0,48	0,06	0,03	6,27
85	M	97,5	97,6	97,6	98,7	10,4	0,21	1,03	0,04	0,05	18,1
87	F	99,1	99,3	99,2	99,4	6,41	0,56	0,11	0,13	0,15	10,5
89	M	99,1	99,9	99,2	99,0	3,28	0,71	0,18	0,05	0,03	8,44
90	M	99,3	99,8	99,7	99,8	0,35	0,62	0,06	0,15	0,19	0,01

>90 90-60 60-40 40-20 20-10 <10 **% Positive population**

Fig. 1 Characterization of bone marrow MSCs. **A**) Cummulative proliferation of MSCs during 6 passages in vitro. **B-C**) Tri-lineage differentiation potential and proportion of senescence-associated beta-galactosidase positive cells. Individual MSC responses are summarized in the table (**B**). Donor responses were evaluated qualitatively as high (+++), positive (++), low (+) and negative (-). Representative images of three-lineage differentiation and positive beta-galactosidase staining are shown for donors F20 and M90 (**C**). Insets represent cultures in control media. Images for all donors are presented in Fig. S1A. **D**) Expression levels of surface antigens associated with MSCs. Individual flow cytometry charts for all donors are presented in Fig. S1B

the isotype controls IgG-PE (Cat. No. 555749) and IgG-FITC (Cat. No. 555786), all from BD Biosciences (San Jose, USA). In addition, antibodies against CD105 (Cat. No. ab53321, Abcam, Cambridge, United Kingdom), CD14 and CD45 (Cat. Nos. 21279143 and 21270453, ImmunoTools, Friesoythe, Germany), CD34 (Cat. No. IM1870, Beckman Coulter, Brea, USA) and HLA-DR (Cat. No. 12-9952-4, eBioscience, San Diego, USA) were used. After staining, cells were washed, resuspended in blocking buffer and immediately analyzed using the Cytoflex flow cytometer and CytExpert software (Beckman Coulter). Positive expression of surface markers was determined using a combination of fluorescence minus one and isotype controls. For the negative controls, the gates were set to 1%.

Tri-lineage differentiation potential was determined in monolayer and pellet cultures, as previously reported [30, 34], using cells from passages 3 to 5. For osteogenic differentiation, cells were seeded in 24-well plates at a density of 5000 cells/cm^2 and cultured in osteogenic medium consisting of DMEM-hg supplemented with 10% FBS, 1% pen-strep, 2 mM L-glutamine, and an osteogenic supplements 10 nM dexamethasone, 50 µM ascorbic acid-2-phosphate and 10 mM ß-glycerophosphate. For adipogenic differentiation, the cells were seeded in 24-well plates at a density of 7400 cells/cm^2 (a higher seeding density provided an additional adipogenic stimulus) and cultured in an adipogenic medium, consisting of DMEM-hg supplemented with 10% FBS, 1% pen-strep, 2 mM L-glutamine and adipogenic supplements 0.5 mM IBMX, 60 µM indomethacin, 0.5 µM hydrocortisone and 1 µM dexamethasone. Control cultures for osteogenic and adipogenic differentiation were seeded in 24-well plates at a density of 5000 cells/cm^2 and cultured in MSC growth medium without bFGF. The cells were inspected regularly and harvested after 25–28 days of culture before the monolayers detached due to cell overgrowth. Osteogenic and adipogenic differentiation was assessed according to standard procedures for Alizarin Red staining of calcium deposits and Oil Red O staining of lipid accumulations. The differentiation potential was qualitatively assessed as high (+++), positive (++), low (+) and negative (-). For correlation analysis, high differentiation potential was assigned value 3, positive potential value 2, low potential value 1 and negative potential value 0. For

combined differentiation rank, the three differentiation ranks were summed-up.

For chondrogenic differentiation, 250,000 cells were transferred to microcentrifuge tubes and centrifuged at 300 x g for 5 min. The resulting cell pellets were either cultured in chondrogenic medium consisting of DMEM-hg supplemented with 1% pen-strep, 1% ITS-X, 100 µg/ml sodium pyruvate, 40 µg/ml L-proline, 100 nm dexamethasone, 50 µg/ml ascorbic acid-2-phosphate and 10 ng/ml TGF-β3, or in MSC growth medium without bFGF as a control. After 4 weeks of culture, the pellets were harvested and processed for histologic analysis as described in the following section.

Senescence was determined in cells of passage 5. The cells were seeded in three replicates in 12-well plates at a density of 5000 cells/cm2. After 2–3 days, when the cultures had reached 30–50% confluence, senescence was determined using senescence β-galactosidase staining kit (Cell Signaling Technology, Danvers, USA), according to the manufacturer's instructions. The stained cultures were imaged using an inverted microscope (Primovert) mounted with a digital camera (AxioCam ICc5, Zeiss, Oberkochen, Germany). Six non-overlapping fields were imaged for each well, and the number of senescent cells and the total number of cells were counted independently by two investigators. Senescence was expressed as the percentage of beta-galactosidase-positive cells out of the total number of cells.

Preparation of conditioned media from hiPSC-MPs and bone marrow-derived MSCs

hiPSC-MPs were derived in our previous study (line 1013 A) and showed a strong growth and trilineage differentiation potential, an expression profile of surface antigens similar to that of bone marrow-derived MSCs, and a normal karyotype [30]. The cells were thawed, seeded in tissue culture flasks pre-coated with 0.1% gelatin in tissue culture water and cultured in a medium consisting of KO-DMEM supplemented with 10% Hyclone-FBS, 1% pen-strep, 2 mM GlutaMAX, 0.1 mM non-essential amino acids, 0.1 mM β-mercaptoethanol and 1 ng/ml bFGF (Thermo Fisher Scientific). For CM preparation, hiPSC-MPs of passages 7–9 were seeded at a density of 10,000 cells/cm^2 and cultured up to 80% confluent. Cultures were washed twice with PBS and incubated in DMEM-hg with 1% pen-strep for 48 h. CM from different flasks was then collected, pooled, filtered and stored in aliquots at -80 °C. After CM collection, the cells in the different flasks were counted to determine comparable cell numbers. Control medium (CTRL) was prepared according to the same protocol in the absence of cells. Two large pools of hiPSC-MP-CM and CTRL medium were merged and used in all experiments except for evaluating the effects of prolonged hiPSC-MP cultivation and predifferentiation, in which separate CTRL and CM were prepared from subconfluent hiPSC-MP cultures. CM was also prepared from bone marrow-derived MSCs from three donors (M22, F71, F85) using the same conditioning protocol as described for hiPSC-MPs.

To investigate the effects of prolonged cultivation and pre-differentiation, CM was prepared from hiPSC-MPs cultured in either growth medium (d14-CM) or osteogenic medium (d14OST-CM) for 14 days. Osteogenic and growth medium were composed as described above for MSC characterization studies, except that the dexamethasone concentration in the osteogenic medium was increased to 1 µM, as previously reported for osteogenic differentiation of hiPSC-MPs [30], and the growth medium did not contain bFGF. Proliferation (DNA content) and alkaline phosphatase (ALP) activity were assessed at the beginning of conditioning in parallel hiPSC-MP cultures seeded in 24-well plates to confirm early osteogenic differentiation (see following sections). Osteogenic differentiation was further verified by staining for ALP activity (Leukocyte Alkaline Phosphatase Kit, Sigma-Aldrich) according to the manufacturer's instructions.

Effect of conditioned media on adult/aged bone marrow-derived MSC osteogenesis

Different types of CM and treatments have been used to investigate the effects of CM on osteogenic differentiation of bone marrow-derived MSCs (see below).

Duration of hiPSC-MP-conditioned medium supplementation to enhance osteogenic differentiation

The effect of hiPSC-MP-CM on early osteogenic differentiation was tested with passage 1 MSCs in monolayer cultures. MSCs were seeded in 96-well plates at a density of 8000 cells/cm^2 in DMEM-hg containing 10% FBS, 0.1% pen-strep and 2 mM L-glutamine to ensure uniform seeding. After 24 h, the medium was replaced with CTRL and CM media freshly supplemented with 10% FBS, 0.1% pen-strep and 2 mM L-glutamine. In addition, the CTRL+O and CM+O groups were formed by adding osteogenic supplements: 10 nM dexamethasone, 50 µM ascorbic acid-2-phosphate and 10 mM ß-glycerophosphate.

To assess the duration of CM supplementation, cultures were either maintained in CM media and controls for 14 days, with complete media changes every 2–3 days (tested with MSCs from all 13 donors). Alternatively, short-term CM supplementation was tested (using MSCs from donors F71 and M89), in which MSC cultures were incubated in CTRL, CM, CTRL+O and CM+O media for three days, and then switched to regular control and osteogenic media (without CM or CTRL) for the remaining 14 days of culture. In parallel groups, the three-day

supplementation was repeated in the second week (days 7–10). Cultures were harvested after 7 and 14 days to determine proliferation (DNA content) and ALP activity.

For gene expression analysis, MSCs (donors M22, F71, M73, F87, M89 and M90) were seeded in 24-well plates at a density of 5000 cells/cm^2, cultured in CTRL, CM, CTRL+O and CM+O media for 14 days, harvested in TRI Reagent® and stored at -80 °C until analysis.

Due to frequent overgrowth and detachment of monolayer cultures between the second and third week of culture in preliminary experiments, the effects on late markers of osteogenesis were tested in pellet cultures, as previously reported [30, 34], using passage 3 MSCs. Pellets were prepared from ~450,000 MSCs (donors F71 and M89) as described above for chondrogenic differentiation and incubated in CTRL, CTRL+O CM and CM+O media for 6 weeks, with complete media changes every 2–3 days. At the end of the culture, the pellets were harvested and processed for histological analysis as described in the following section.

Effect of hiPSC-MP-conditioned medium dose

For the dose-response experiments, CM and CTRL media were successively concentrated using VivaSpin 20 ultrafiltration devices with 30 kDa and 3 kDa MWCO (Sartorius, Göttingen, Germany) to obtain a 20-fold concentrated CM fraction. Dilution series of the concentrated CM and CTRL media (1:1, 1:2, 1:4 and 1:8 dilutions) were prepared using fresh KO-DMEM supplemented with 10% FBS, 0.1% pen-strep and 2 mM L-glutamine. In parallel, CM and CTRL dilution series were prepared supplemented with osteogenic supplements. CM and CTRL dilution series with/without osteogenic supplements were tested in 96-well plates with monolayer cultures of MSCs (donors F71, F85 and M89). Cultures were continuously supplemented for 14 days as described above for CM and harvested at week 1 and 2 to determine proliferation (DNA content) and ALP activity.

Effects of cell source and hiPSC-MP prolonged cultivation/osteogenic differentiation on conditioned medium stimulatory activity

The effects of hiPSC-MP-CM were compared with the effects of CM derived from MSCs from three donors (M22, F71 and M85) using responding MSCs from two donors (F71 and F85).

To assess the effects of prolonged cultivation or predifferentiation of hiPSC-MPs on CM functionality, CTRL, CM, d14-CM and d14OST-CM media with or without osteogenic supplements were tested with MSCs from donor F85. MSCs of passage 1 were seeded in monolayer cultures and continuously supplemented with different CM types for 14 days as described above, after which proliferation (DNA content) and ALP activity were determined.

DNA content determination

Proliferation of bone marrow-derived MSC in response to different CM and control media was analysed using the Molecular Probes™ CyQUANT™ Cell Proliferation Assay (Thermo Fisher Scientific) according to the manufacturer's instructions. Briefly, cultures were harvested in 96-well plates, washed once with PBS and cell monolayers were stored at -80 °C until analysis. The plates were thawed to room temperature, then 200 µl of freshly prepared fluorescent reagent was added to the wells and incubated for 5 min in the dark. The fluorescence was measured at 485/520 nm. The DNA concentration of the samples was determined using a standard curve prepared in parallel with the DNA standard provided with the assay kit.

To assess the proliferation of hiPSC-MPs after 14 days of culture in 24-well plates in growth and osteogenic medium (before the start of conditioning), DNA content was determined as previously described [35]. Briefly, cultures were harvested in the well plates, washed once with PBS and digested overnight at 60 °C in a buffer containing 150 mM NaCl, 55 mM Na citrate * $2H_2O$, 20 mM EDTA * 2 H_2O, 0.2 M NaH_2PO_4 * 1 H_2O, 10 mM EDTA * 2 H_2O, 6 U/mL papain, and 10 mM cysteine in ddH_2O (with a pH of 6.0). The digested samples were collected, centrifuged at 300 × g for 5 min, and the DNA content of the supernatant was determined using Hoechst 33,342 dye in assay buffer (2 M NaCl, 50 mM NaH_2PO_4, pH 7.4). Samples were incubated for 5 min at 37 °C in the dark with slow shaking, and fluorescence was measured at 355/460 nm. The DNA concentration of the samples was determined using a standard curve generated with calf thymus DNA solutions of known concentrations.

Alkaline phosphatase activity determination

To determine ALP activity, cell monolayers were washed in 96-well plates and stored as described above for DNA content. After thawing to room temperature, ALP activity was determined using Alkaline Phosphatase Yellow (pNPP) Liquid ELISA substrate (P7998, Sigma-Aldrich), as previously reported [36]. Briefly, 100 µl of the substrate was added to the wells, and the plates were incubated at 37 °C until yellow color development. The reaction was stopped by adding 100 µl of 0.1 M NaOH, the reaction time was recorded, and the absorbance was determined at 405 nm. ALP activity was determined using a standard curve generated with p-nitrophenol solutions of known concentrations.

ALP activity of hiPSC-MPs after 14 days of culture in 24-well plates in growth and osteogenic medium (at the beginning of conditioning) was determined as previously

described [35]. Cultures were harvested, washed and lysed in a solution containing 0.5% Triton X-100 in 0.5 M 2-amino-2-methyl-1-propanol buffer with 2 mM MgCl2 (pH 10.3). The lysed samples were centrifuged at 300 x g for 5 min and the ALP activity of the supernatant was determined by adding the 0.02 M p-nitrophenyl phosphate substrate solution to the extracted supernatant and incubating at 37 °C until yellow color development. The reaction was stopped by adding 0.2 M NaOH stop solution and the reaction time was recorded. The absorbance was measured at 405 nm and the ALP activity was determined using a standard curve generated with p-nitrophenol solutions of known concentrations.

Gene expression analyses

MSCs grown for 14 days in 24-well plates in CM and control media were harvested in TRI Reagent® and total RNA was isolated according to the manufacturer's instructions. The isolated RNA was treated with amplification-grade DNase I, and 300–800 ng of RNA was reverse transcribed into cDNA with the GoScript™ Reverse Transcription System 100 (Promega, Wisconsin, USA) using random hexamer primers. Real-time PCR was performed using the CFX96 Real-Time PCR Detection System (Bio-Rad Laboratories, Hercules, USA). 2 µL of cDNA was added to a 25 µL reaction containing the TaqMan® Universal PCR Master Mix and one of the TaqMan® gene expression assays (Thermo Fisher Scientific) for alkaline phosphatase (ALP, Hs01029144_m1), ostepontin (OPN, Hs00959010_m1), bone sialoprotein (BSP, Hs00173720_m1), and glyceraldehyde 3-phosphate dehydrogenase (GAPDH, Hs02786624_g1) (URL links to assay information are provided in Suppl. Data File 1). Standard cycling conditions were used: 95 °C for 10 min, followed by 40 cycles of 95 °C for 15 s (denaturation) and 60 °C for 60 s (annealing and extension). Results were exported with CFX Manager 3.1 (Bio-Rad Laboratories, California, USA) and analyzed in Excel (Microsoft, Redmond, USA) using the ΔΔCt method. The expression levels of osteogenic target genes were normalized to the expression level of the housekeeping gene GAPDH as in our previous studies.

Histological and immunohistochemical analyses

The collected pellets were washed with PBS and fixed in 4% phosphate-buffered formaldehyde (Roti®-Histofix 4%, P087.3, Carl Roth, Karlsruhe, Germany) for 24 h. Samples were then rinsed, dehydrated in an increasing series of EtOH concentrations and embedded in paraffin using a vacuum infiltration device (Tissue Tek, Sakura Finetek, Nagano, Japan). 4 µm thin sections were cut with a microtome (Microm HM 355 S, Thermo Fisher Scientific), placed on glass slides and stored overnight at 37 °C to ensure optimal adhesion of the sections to the glass slides.

Immunohistochemical staining was performed to determine the presence of collagen type II. Sections were rehydrated in a descending EtOH series. Antigen retrieval was performed by pepsin treatment (Pepsin Reagent Antigen Retriever, R2283, Merck KGaA, Darmstadt, Germany) for 10 min at 37 °C in a humidified chamber. The sections were then incubated with a primary antibody against collagen type II (MS 306-P1; Collagen II Ab-3 (clone 6B3), mouse monoclonal antibody, Thermo Fisher Scientific) for one hour at RT. After washing, the samples were incubated with a secondary HRP anti-mouse antibody (Bright Vision poly HRP-Anti-Mouse IgG, VWRKDPVM110HRP, ImmunoLogic, Duiven, The Netherlands) for 30 min at RT. The signal was detected using the NovaRed® HRP peroxidase substrate kit (ImmPACTTMNova RedTM, SK4805, Vector Laboratories, Burlingame, USA) according to the manufacturer's instructions, and cell nuclei were stained with Haemalaun.

To visualize pellet morphology and growth in CM and control media with/without osteogenic supplements, sections were stained with hematoxylin and eosin, and pellet mineralization was assessed using the standard von Kossa staining procedure.

Determination of TGFβ–1 content

The concentrations of TGFβ–1 in CTRL, CM, d14-CM and d14OST-CM media samples were determined with the Quantikine® ELISA kit (R&D Systems, Minneapolis, USA) according to the manufacturer's instructions using a standard curve generated with standards of known concentrations included in the kit.

Proteomic analysis

Samples of CTRL, CM and d14-CM from three independent preparations were collected and stored at -80 °C until mass spectrometry (MS) proteomic analysis. Detailed MS analysis procedures are described in Suppl. Data File 1. Briefly, proteins were precipitated from the CM with a mixture of dichloromethane and methanol, followed by a series of centrifugation steps to remove the supernatant, leaving a pellet that was then air-dried. The pellets were dissolved in 50 µl of 50 mM triethylammonium bicarbonate (Sigma Aldrich) containing 0.1% RapiGest SF (Waters, Milford, USA) for protein solubilization. Protein concentrations were measured using a nano spectrophotometer (DS-11, DeNovix, Wilmington, USA). The proteins were then reduced, alkylated, and digested with MS-grade trypsin (Thermo Fisher Scientific) before being stored at -80 °C until further analysis. For nanochromatographic separation, a Nano-RSLC UltiMate 3000 system (Thermo Fischer Scientific) was used,

employing a PepMap C18 trap-column (Thermo Fischer Scientific) for sample loading and desalting and a 200 cm C18 µPAC column (PharmaFluidics, Ghent, Belgium) for separation of the digested proteins. The separation used a cooled aqueous loading phase and a gradient elution in which two mobile phases were mixed to improve the capture of hydrophilic analytes and optimize peptide separation. Peptides were then analyzed using both UV at 214 nm (3 nl UV cell) and a Q-Exactive Orbitrap Plus mass spectrometer (both Thermo Fisher Scientific). The collected raw MS data were searched against the human UniProt protein database (February 2023 version) using FragPipe 21.1 (Nesvilab, Michigan, USA; https://fragpipe.nesvilab.org/) [37]. Statistical analysis and visualization was performed using Perseus version 1.6.5.0 (Cox lab, Martinsried, Germany; https://cox-labs.github.io/coxdocs/perseus_instructions.html) [38]. The program String (https://string-db.org/) [39] was used to investig ate the biological relationship between the differentially expressed proteins and functional enrichments. The mass spectrometry proteomics data have been deposited to the ProteomeXchange Consortium [40] via the PRIDE partner repository with the dataset identifier PXD052766 [41].

Statistical analyses

Data are presented either as individual values, or as a combination of mean ± SD with individual values. Normal distribution of the data was first tested using the Shapiro-Wilk test. Data showing a normal distribution were tested using t-test, one-way ANOVA or two-way ANOVA, followed by Tukey's multiple comparison test. Data that did not show a normal distribution were analysed using the Friedman test followed by Dunn's test for multiple comparisons. Correlations between specific proliferation rate, senescence-associated beta-galactosidase expression (middle) and MSC donor age were evaluated using Pearson's correlation coefficient. Correlations between osteogenesis, chondrogenesis, adipogenesis, trilineage potential and MSC donor age were evaluated using Spearman's rank correlation coefficient. The significance level was set at 0.05 for all analyses. The analyses were performed using Microsoft Excel (Redmond, USA) for the t-test and GraphPad Prism 10 software (GraphPad Software, San Diego, USA). The type of analysis, number of samples and significant differences between groups are indicated in the legends of each figure. Detailed statistical analyses of the proteomic data are provided in Suppl. Data File 1.

Results

Primary human bone marrow-derived MSCs show a decrease in proliferation and differentiation potential and different degrees of senescence with increasing chronological age of the donors

We isolated MSCs from the femoral bone marrow of 11 patients who had undergone hip replacement surgery (M43-M90) and from bone marrow mononuclear cells from 2 additional donors (F20, M22) from a commercial source (Fig. 1, Fig. S1, Fig. S2). Overall, we observed a negative correlation between MSC proliferation rate and chronological age of the donor (Fig. 1A, Fig. S2A). We also observed a positive correlation between the senescence level and specific proliferation rate of MSCs (Fig. 1B, Fig. S2A). The fastest proliferation was observed in MSCs from young adult donors F20 and M22 and from donors F44 and M73, which had a low proportion of senescent beta-galactosidase positive cells (0.5-5%, Fig. 1B, Fig. S1A), whereas the slowest proliferation in MSCs was observed from donors F78 and M90, which had the highest proportion of senescent beta-galactosidase-positive cells (34% and 39%, respectively, Fig. 1B, Fig. S1A). In general, the proportion of senescence-associated beta-galactosidase-positive cells varied among MSCs isolated from donors of different ages (Fig. S2A).

A strong potential for osteogenic differentiation was observed in MSCs from donors F20 and M22, and a low potential for osteogenic differentiation in MSCs from donors M73 and F85 (Fig. 1B, C, Fig. S1A, Fig. S2B). All other MSCs showed no osteogenic differentiation potential, and the negative correlation between the MSC donor age and osteogenic potential was not significant (Fig. S2B). MSCs from young adult donor F20 showed the strongest chondrogenic differentiation potential, and MSCs from various adult and aged donors showed positive or low chondrogenic potential, with no correlation to MSC donor age (Fig. 1B, C, Fig. S1, Fig. S2B). However, the pellet size and the area of extracellular matrix stained positive for collagen type II were smaller in adult and aged donors compared to MSCs from donor F20 (Fig. S1). Interestingly, MSCs from donor M22 showed no chondrogenic differentiation potential in vitro. The adipogenic differentiation potential was highest in MSCs from donors F20, M22 and M43 and moderate in cells from donor M73 (Fig. 1B, C, Fig. S1). MSCs from all other donors showed low adipogenic differentiation potential, indicating the significant negative correlation between adipogenic potential and MSC donor age (Fig. S2B). Overall, our data suggest that the proliferation and trilineage differentiation potential of bone marrow-derived MSCs significantly decreases with increasing chronological age of the donors (Fig. S2).

Expression of the MSC-associated surface antigens CD44, CD73, CD90 and CD105 was detected in >98%

of the cell population in all donors, while CD14, CD31, CD34 and CD45 were expressed in < 5% of the cell population (Fig. 1D, Fig. S1B). Expression of CD146 varied between donors and was highest in cells from donors M22 and M73 (75% and 70% of the cell population, respectively). Expression of HLA-DR was detected in 10–20% of cells from 5 donors, and MSCs from donor M73 had a high proportion of HLA-DR-positive cells (61% of the total population).

Conditioned medium of hiPSC-MPs enhances early osteogenic differentiation of aged bone marrow-derived MSCs

First, we investigated the effect of short-term supplementation with hiPSC-MP-CM on osteogenic differentiation of MSCs from donors F71 and M89 (Fig. S3). It was found that neither 3-day supplementation with CM during the first week of culture nor repeated 3-day supplementation with CM during the first and second week of culture reproducibly increased DNA content (Fig. S3A, B, left graphs) and ALP activity (Fig. S3C, D, left graphs) compared to the control. In contrast, continuous 14-day supplementation of osteogenic cultures with CM resulted in significantly higher DNA content (Fig. S3A, B, right graphs) and ALP activity (Fig. S3C, D, right graphs) compared to the control for both donors. (Fig. S3). Based on these results, we tested the response to continuous 14-day CM supplementation with MSCs from all 13 donors (Fig. 2). We found a significantly higher increase in DNA content in osteogenic cultures grown in CM compared to CM and control groups without osteogenic supplementation (Fig. 2A). In the osteogenic groups, we observed a trend towards increased DNA content in CM compared to the control, which was not statistically significant. Evaluation of donor-specific MSC responses in osteogenic cultures showed a significantly increased DNA content in MSC from 8 donors cultured in CM compared to control, while MSC from 5 donors showed a comparable DNA content (Fig. 2B).

The increase in ALP activity after 14 days of culture was significantly higher in the osteogenic groups than in the non-osteogenic groups. In the osteogenic groups,

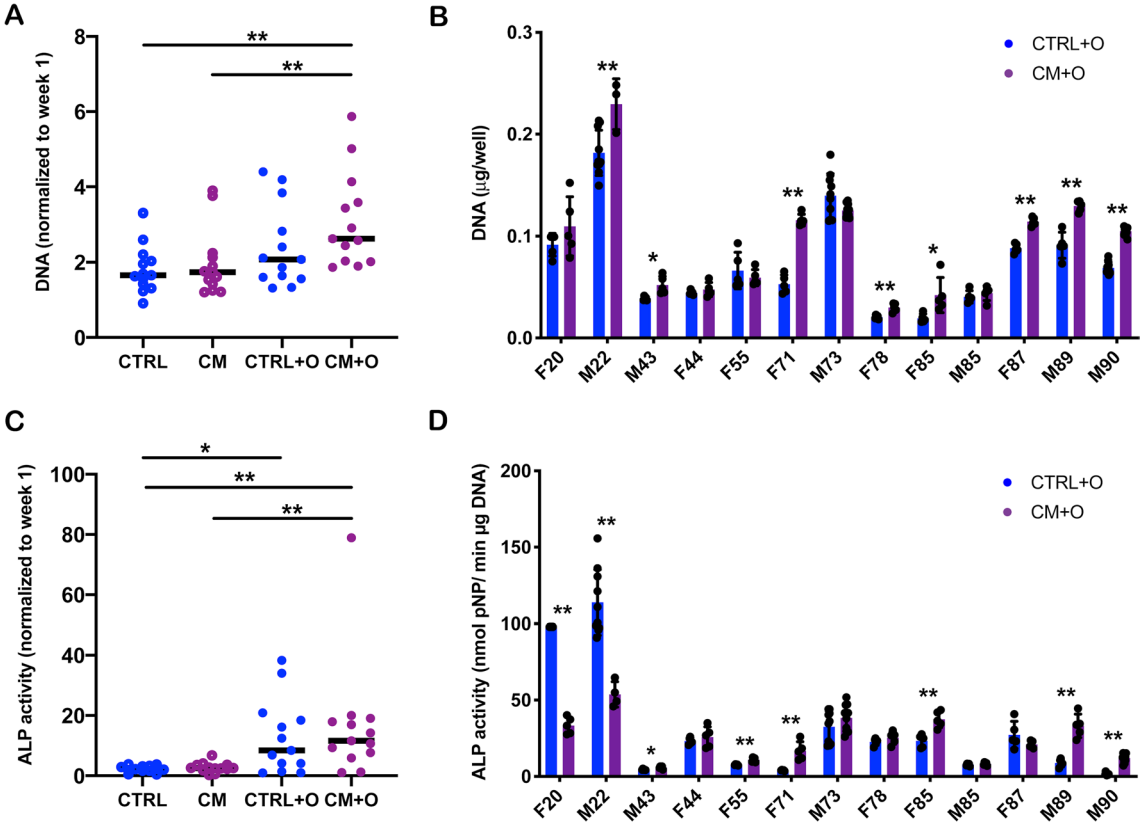

Fig. 2 hiPSC-MP-conditioned medium enhances early osteogenic differentiation of bone marrow MSCs. **A-B**) DNA content and **C-D**) ALP activity quantification after 14 days of continuous supplementation with CM or control medium under non-osteogenic and osteogenic conditions. Data is shown for MSCs from all 13 donors relative to week 1 (**A**, **C**) and individual donor responses are shown for cultures under osteogenic conditions (**B**, **D**). Group labels: CTRL—control, CM—conditioned medium, CTRL + O—control with osteogenic supplements, CM + O—conditioned medium with osteogenic supplements. Data represents individual values with mean (**A**, **C**, $n = 13$) or a combination of mean ± SD with individual values (**B**, **D**, $n = 3–10$). Statistically-significant differences between the groups were evaluated using Friedman test followed by Dunn's multiple comparisons test (**A**, **C**) or unpaired t-test (**B**, **D**), and are marked as: *$p < 0.05$; **$p < 0.01$

a trend towards increased ALP activity was observed with hiPSC-MP-CM supplementation compared to the control (Fig. 2C). However, continuous 14-day CM supplementation did not replace the requirement of adding osteogenic supplements, as CM and CTRL treatments were comparable. Evaluation of donor-specific MSC responses under osteogenic conditions showed significantly increased ALP activity for MSC from 6 donors in CM compared to control, while MSC from 5 donors showed comparable ALP activity between the two groups (Fig. 2D). Interestingly, MSCs from 2 of the youngest donors showed a significant decrease in ALP activity in CM compared to control (Fig. 2D).

After 14 days of culture in hiPSC-MP-CM, a trend towards increased ALP gene expression was observed compared to the control medium without osteogenic supplements. Osteogenic supplementation of the control medium resulted in a significant increase in ALP gene expression compared to the non-osteogenic controls, while the CM group under osteogenic conditions showed lower ALP expression compared to the control (Fig. S4A). Similarly, CM supplementation resulted in decreased gene expression of the late markers osteopontin (Fig. S4B) and bone sialoprotein (Fig. S4C) after 14 days of culture. Continuous 6-week culture of MSC pellets in CM with or without osteogenic supplements also did not result in increased pellet mineralization (Fig. S4D). Overall, our data suggest that CM can enhance early, but not late, osteogenic differentiation of adult/aged bone marrow-derived MSCs.

Bone marrow-derived MSCs response to hiPSC-MP-conditioned medium is dose-dependent

The response of bone marrow-derived MSCs to hiPSC-MP-CM dilution series was tested in three donors (F71, F85 and M89) after 14 days of continuous supplementation. MSCs from donors F71 and F85 showed a significant increase in DNA content with increasing CM concentration compared to the control, both under non-osteogenic and osteogenic conditions (Fig. 3A). In contrast, M89 cells in the CM groups showed an overall lower DNA content compared to the control, both under non-osteogenic and osteogenic conditions. However, we observed a trend towards increased DNA content with increasing CM concentration. ALP activity increased with increasing CM concentration in MSCs from all three donors and was significantly higher in CM than in CM dilutions and in the control, both under non-osteogenic and osteogenic conditions (Fig. 3B). Overall, we found a dose-dependent response of proliferation and osteogenic differentiation

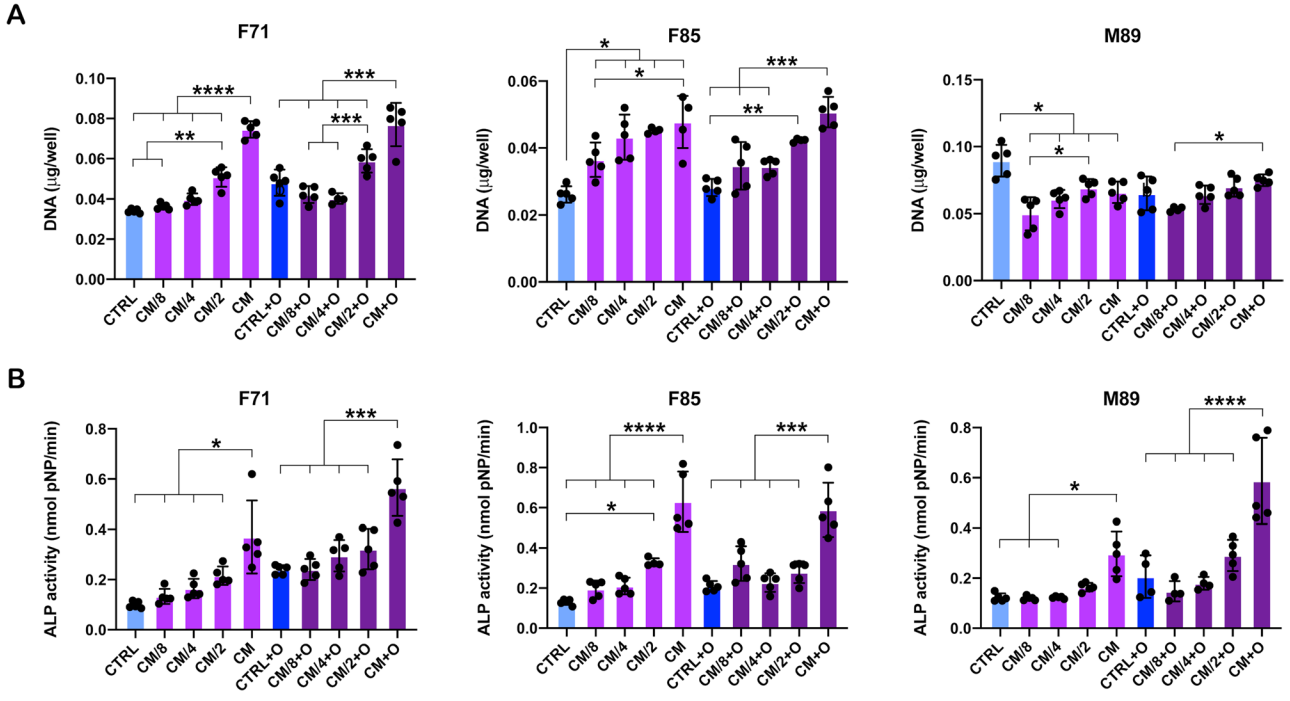

Fig. 3 Osteogenic response of bone marrow MSCs to hiPSC-MP-conditioned medium is dose-dependent. **A**) DNA content and **B**) ALP activity quantification after 14 days of continuous supplementation of MSCs (donors F71, F85, M89) with increasing doses of CM or control medium under non-osteogenic and osteogenic conditions. Group labels: CTRL—control, CM/8, CM/4, CM/2—conditioned medium dilutions 1:8, 1:4, 1:2, CM—conditioned medium, CTRL + O—control with osteogenic supplements, CM/8 + O, CM/4 + O, CM/2 + O—conditioned medium dilutions 1:8, 1:4, 1:2 with osteogenic supplements, CM + O—conditioned medium with osteogenic supplements. Data represents a combination of mean ± SD with individual values ($n = 4–5$). Statistically-significant differences between the groups were evaluated using one-way ANOVA followed by Tukey's multiple comparisons test and are marked as: *<0,05; **<0,01; *** <0,001; ****<0,0001

of aged bone marrow-derived MSCs to hiPSC-MP-CM supplementation. In these experiments, CM supplementation alone replaced the need for osteogenic supplements. However, the highest proliferation and osteogenic differentiation were found in CM group under osteogenic stimulation.

hiPSC-MP-conditioned medium shows stronger stimulatory activity compared to conditioned medium from bone marrow-derived MSCs

Next, we compared the osteogenic differentiation-stimulating activity of hiPSC-MP-CM with conditioned media prepared from bone marrow-derived MSCs from donors M22, F71 and F85. In F71 cells, a significantly higher DNA content was observed for all conditioned media compared to the control, both under non-osteogenic and osteogenic conditions (Fig. 4A). For F85 cells, all conditioned media resulted in significantly higher DNA content compared to the control under osteogenic conditions. When comparing CM cell sources, hiPSC-MP-CM supplementation resulted in significantly higher DNA content compared to all MSC-conditioned media for both donors tested under osteogenic conditions. Under non-osteogenic conditions, hiPSC-MP-CM and M22-CM resulted in a significantly lower DNA content compared to CM from F71 and F85 cells.

ALP activity was significantly higher in MSCs from both donors in all CM groups compared to controls

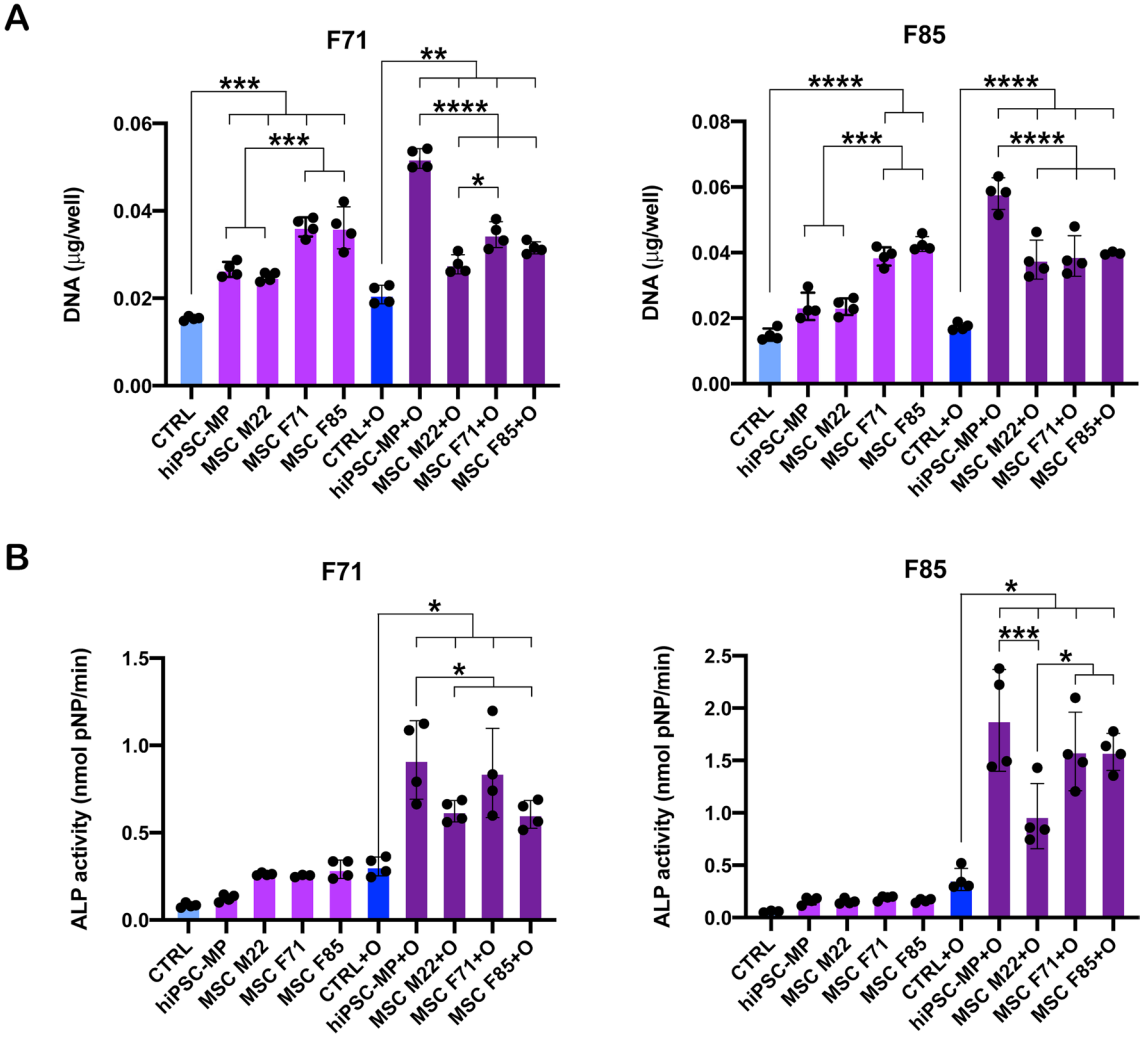

Fig. 4 hiPSC-MP-conditioned medium outperforms bone marrow MSC-conditioned media. **A**) DNA content and **B**) ALP activity quantification after 14 days of continuous supplementation of MSCs (donors F71, F85) with hiPSC-MP-CM, CM from MSCs F20, F71 and F85 or control medium under non-osteogenic and osteogenic conditions. Group labels: CTRL—control, hiPSC-MP—conditioned medium from hiPSC-MPs, MSC M22/F71/F85—conditioned medium from M22/F71/F85 cells, CTRL + O—control with osteogenic supplements, hiPSC-MP + O—conditioned medium from hiPSC-MPs with osteogenic supplements, MSC M22 + O/F71 + O/F85 + O—conditioned medium from M22/F71/F85 cells with osteogenic supplements. Data represents a combination of mean ± SD with individual values ($n = 3–4$). Statistically-significant differences between the groups were evaluated using one-way ANOVA followed by Tukey's multiple comparisons test and are marked as: *<0,05; **<0,01; *** <0,001; ****<0,0001

under osteogenic conditions (Fig. 4B). No significant differences in ALP activity were observed under non-osteogenic conditions. With respect to CM cell source, ALP activity showed the highest values when MSCs were supplemented with hiPSC-MP-CM. In F71 cells, significant differences were observed between hiPSC-MP-CM and CM from M22 and F85 cells. In F85 cells, significant differences were observed with M22-CM, which had lower ALP activity than other conditioned media groups. Overall, hiPSC-MP-CM showed a stronger enhancement of aged bone marrow-derived MSC early osteogenic differentiation compared to CM from bone marrow-derived MSCs.

Prolonged cultivation under non-osteogenic conditions increases the stimulatory activity of hiPSC-MP-conditioned medium

In previous experiments, hiPSC-MPs were cultured to subconfluence prior to CM preparation. Next, we investigated whether prolonged 14-day cultivation (d14-CM) or pre-differentiation of hiPSC-MPs into the osteogenic lineage (d14OST-CM) could influence the stimulatory activity of the medium. We verified the osteogenic differentiation of hiPSC-MPs, which showed significantly increased DNA content (Fig. S5A) and ALP activity (Fig. S5B) after 14 days of culture under osteogenic conditions compared to non-osteogenic conditions. Furthermore, osteogenic differentiation was confirmed by positive ALP activity staining (Fig. S5C).

Supplementation of F85 MSCs with d14-CM and d14OST-CM resulted in significantly higher DNA content compared to supplementation with regular CM when the MSCs were grown under non-osteogenic conditions (Fig. 5A). Under osteogenic conditions, all CM groups resulted in significantly higher DNA content compared to the control. However, the DNA content was highest in the d14-CM group and was significantly different from the d14OST-CM and CM groups.

ALP activity of F85 cells was significantly higher in the d14OST-CM group compared to the CM and control groups under non-osteogenic conditions (Fig. 5B). Under osteogenic conditions, the d14-CM group exhibited the highest levels of ALP activity overall, which was significantly different from those of the d14OST-CM, regular CM and control groups. Taken together, these data suggest that 14 days of prolonged cultivation enhances the potential of hiPSC-MP-CM to stimulate osteogenic differentiation of bone marrow-derived MSC. We next evaluated concentrations of TGFβ–1, one of the major growth factors regulating osteogenesis and bone homeostasis, and previously identified in the MSC secretome (Fig. 5C). Interestingly, concentration profile of TGFβ–1 in the three different CM groups and the control medium corresponded to the response profiles of DNA content and ALP activity, with the highest TGFβ–1 levels found in the d14-CM, which had the highest increase in DNA content and ALP activity.

Enhanced d14-CM stimulatory activity is associated with a distinct profile of protein components that form a highly interconnected protein associations network

To identify CM protein components associated with improved functionality, we performed a comparative proteomic analysis of d14-CM (the group resulting in highest MSC responses), regular CM and conditioning control medium. A total of 472 proteins were identified in the three groups, with 33 proteins in control medium, 75 proteins in regular CM only, 152 proteins in d14-CM

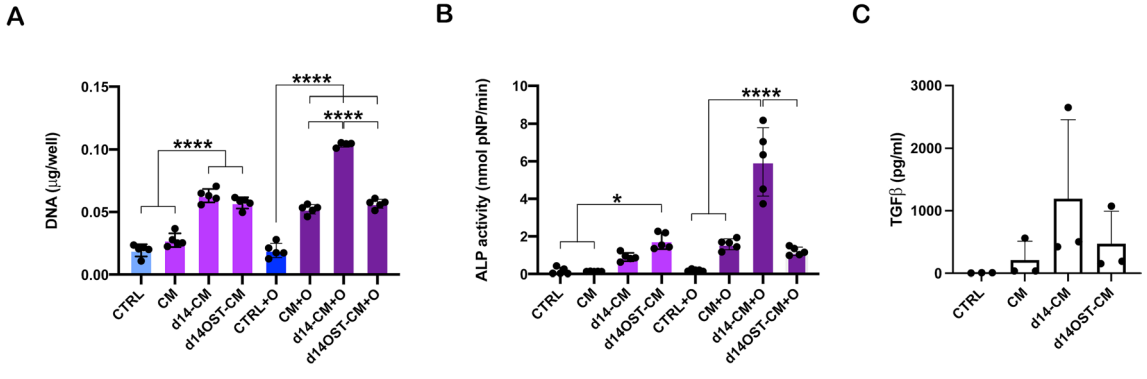

Fig. 5 Prolonged cultivation of hiPSC-MPs under non-osteogenic conditions increases conditioned medium functionality. **A**) DNA content and **B**) ALP activity quantification after 14 days of continuous supplementation of MSCs (donor F85) with regular CM, prolonged cultivation CM, CM from pre-differentiated hiPSC-MPs or control medium under non-osteogenic and osteogenic conditions. **C**) Quantification of TGFβ-1 content. Group labels: CTRL—control, CM—conditioned medium, d14-CM—prolonged cultivation conditioned medium, d14OST-CM—osteogenic pre-differentiation conditioned medium, CTRL + O—control with osteogenic supplements, CM + O—conditioned medium with osteogenic supplements, d14-CM + O—prolonged cultivation conditioned medium with osteogenic supplements, d14OST-CM + O—osteogenic pre-differentiation conditioned medium with osteogenic supplements. Data represents a combination of mean ± SD with individual values ($n = 4–5$ for **A**, **B**; $n = 3$ for **C**). Statistically-significant differences between the groups (**A**, **B**) were evaluated using one-way ANOVA followed by Tukey's multiple comparisons test and are marked as: *<0,05; ****<0,0001

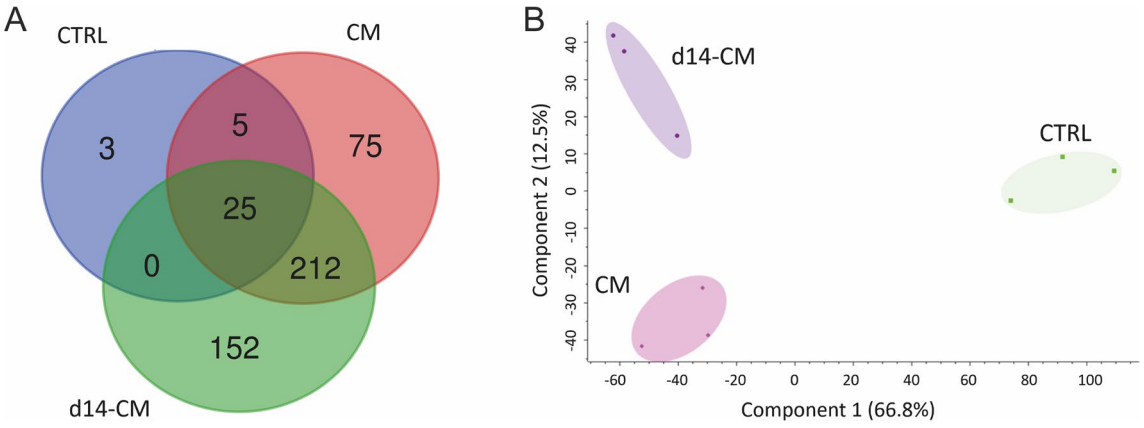

Fig. 6 Proteomic analysis of hiPSC-CM preparations. **(A)** Venn diagram of protein components identified in regular CM, prolonged cultivation d14-CM and control medium ($n=3$). **(B)** Principal component analysis showed that CM, d14-CM and control media form distinct entities. Group labels: CTRL—control, CM—conditioned medium, d14-CM—prolonged cultivation conditioned medium

only, and 212 proteins in the two CM groups only (Fig. 6A, Suppl. Data File 2). Principal component analysis showed that the CM groups and the control medium formed distinct entities (Fig. 6B).

For further quantitative analyses, proteins identified in the control medium were excluded and only the proteins identified in at least 2 of 3 samples per CM group were included. Of the proteins found in both CM groups, 26 proteins were significantly upregulated in d14-CM, including extracellular matrix protein perlecan (HSPG2, 69-fold), actin-binding protein Lasp-1 (50-fold), insulin-like growth factor binding protein 7 (IGFBP7, 42-fold), lysyl oxidase-like 2 (LOXL2, 33-fold), HtrA serine peptidase 1 (HTRA1, 24-fold), thrombospondin 2 (THBS2, 24-fold), protein disulfide isomerase family A member 3 (PDIA3, 24-fold), extracellular matrix protein versican (VCAN, 21-fold) and secreted protein acidic and cysteine-rich (SPARC, 20-fold) (Table 1, Suppl. Data File 3). On the other hand, 8 proteins were significantly downregulated in d14-CM compared to regular CM, including nucleophosmin 1 (NPM 1, 20-fold), stathmin 1 (STMN1, 14-fold), ribosomal protein L12 (RPL12, 11-fold), pentraxin 3 (PTX3, 11-fold) and procollagen C-endopeptidase enhancer (PCOLCE, 10-fold) (Table 1, Suppl. Data File 3).

String network analyses were performed in which the proteins significantly upregulated in d14-CM were grouped with the proteins uniquely identified in d14-CM (Fig. 7) and the proteins significantly upregulated in regular CM were grouped with the proteins uniquely identified in regular CM (Fig. 8). We found that the proteins upregulated/unique in d14-CM formed a highly interconnected associations network with 97 nodes, an average node degree of 7.56, and a PPI enrichment P value of less than 1.0e−16. Two main clusters were observed in the network, which had different functional enrichment terms according to Gene Ontology (GO) analysis. Cluster 1 was strongly associated with actin filament bundle in cellular components; actin-, actin filament- and cytoskeleton protein binding in molecular functions; and actin filament-, actin cytoskeleton- and cytoskeleton organization in biological processes (Fig. 7 left, Suppl. Data File 3). Hub proteins in Cluster 1 included cytoskeleton-associated proteins tropomyosin 1 (TPM1), TPM2 and TPM4, actin-related protein 3 (ACTR3), vasodilator stimulated phosphoprotein (VASP), actin binding LIM and SH3 protein 1 (LASP1), myosin light chain 9 (MYL9), myosin heavy chain 10 (MYH10), actinin alpha 1 (ACTN1), filamin A (FLNA) and others (Table 1).

Cluster 2 was strongly associated with terms extracellular matrix in cellular components; collagen-, growth factor- and extracellular matrix binding and extracellular matrix structural constituents in molecular functions; and negative regulation of angiogenesis in biological processes (Fig. 7 middle, Suppl. Data File 3). Hub proteins in Cluster 2 included periostin (POSTN), fibrillin 1 (FBN1), bone morphogenetic protein 1 (BMP1), SPARC, VCAN, TBHS2, HSPG2, TGFβ–2 (TGFB2) and others (Table 1).

In addition, GAPDH presented as a highly interconnected hub linking the two clusters, and the d14-CM network as a whole included proteins strongly associated with extracellular space in cellular components; cell adhesion molecule- and protein binding and structural molecule activity in molecular functions; and anatomical structure development, developmental process and supramolecular fiber organization in biological processes, as well as many other terms (Fig. 7 right, Suppl. Data File 3).

In contrast, proteins that were upregulated or uniquely present in regular CM formed a less abundant network with 41 nodes with an average node degree of 2.15 and a PPI enrichment P value of 0.000106 (Fig. 8). Two smaller clusters were observed that had different functional GO enrichments. The proteins in cluster 1 were strongly

Table 1 Top upregulated (green) and downregulated proteins (red) in d14-CM compared to regular CM and their presence as hub proteins in string network of functional associations

Gene - protein Name	Fold change d14-CM/CM	Hub	Function	Reference
HSPG2 - perlecan	69	d14 CL2	Ubiquitous matrix stabilizing proteoglycan Roles in angiogenesis, connective tissue development and repair	[42]
LASP1 - LIM and SH3 protein 1	50	d14 CL1	Ubiquious LIM subfamily signaling protein, overexpressed in cancer cells Binds to actin cytoskeleton; has a role in embryonic development	[43]
IGFBP7 - insulin-like growth factor binding protein 7	42	d14 CL2	Member of IGF-binding protein family Induces osteogenic differentiation of bone marrow-derived MSCs	[44]
LOXL2 – lysyl oxidase like 2	33	d14 CL2	Member of lysyl oxidase family Catalyzes cross links in collagen and elastin	[45]
HTRA1 - HtrA serine peptidase 1	24		Member of serine protease family Regulates availability of IGF-like growth factors	[46]
THBS2 – thrombospondin 2	24	d14 CL2	Member of thrombospondin family Mediates cell-cell and cell-matrix interactions, influences bone fracture healing	[47, 48]
PDIA3 - protein disulfide isomerase family A member 3	24		Ubiquious endoplasmic reticulum protein Modulates protein folding, involved in production of ECM	[49, 50]
VCAN - versican	21	d14 CL2	Member of aggrecan/versican proteoglycan family, major component of ECM Involved in cell adhesion, proliferation, migration, angiogenesis	[51]
SPARC - secreted protein acidic and cysteine-rich	20	d14 CL2	ECM protein involved in matrix synthesis, and cell shape changes Required for bone collagen calcification	[52]
BGN - biglycan	15	d14 CL2	Member of small leucine-rich proteoglycan family of proteins Role in bone growth, muscle development and regeneration, and collagen fibril assembly in multiple tissues	[53]
FBN1 – fibrillin 1	12	d14 CL2	Extracellular matrix glycoprotein Component of calcium-binding microfibrils that provide structural support in connective tissue	[54]
IGFBP2 – insulin growth factor binding protein 2	11	d14 CL2	One of six proteins binding insulin growth factors Promotes tumor growth, role in regulation of bone metabolism	[55, 56]
NPM1 - nucleophosmin 1	-20	CL1	Invovled in centrosome duplication, protein chaperoning, and cell proliferation Sequesters tumor supressor ARF	[57]
STMN1- stathmin 1	-14		Member of stathmin family Intracellular relay for signals of the cellular environment, regulates cell proliferation, destabilizes microtubules	[58]
RPL12 - ribosomal protein L12	-11		Component of the 60 S ribosomal subunit Binds directly to 26 S rRNA	[59]
PTX3 - pentraxin 3	-11		Member of pentraxin protein family Induced by inflammatory cytokines, plays a role in angiogenesis and tissue remodeling	[60]
PCOLCE - procollagen C-endopeptidase enhancer	-10	CL2	Ubiquious glycoprotein Mediates enzymatic cleavage of type I procollagen, heightens C-proteinase activity	[61]

d14 CL1 – protein hub in cluster 1 of d14-CM String associations network; d14 CL2 – protein hub in cluster 2 of d14-CM String associations network (shown in Fig. 7). CL1 – protein hub in cluster 1 of CM String associations network; CL2 - protein hub in cluster 2 of CM String associations network (shown in Fig. 8)

associated with the commitment complex and the proteasome core complex in cellular components and with RNA binding in molecular functions (Fig. 8 left, Suppl. Data File 3), and included hub proteins small nuclear ribonucleoprotein D3 polypeptide (SNRPD3), U2 small nuclear RNA auxiliary factor 2 (U2AF2), LSM3 homolog U6 small nuclear RNA and mRNA degradation associated (LSM3), proteasome 20 S subunit beta 2 (PSBM2) and PSBM6, and nucleophosmin 1 (NPM1) (Table 1). Cluster 2 proteins were strongly associated with the collagen-extracellular matrix and the extracellular matrix in cellular components (Fig. 8 middle, Suppl. Data File 3) and included MMP2, COL6A2, COL6A3 and procollagen C-endopeptidase enhancer (PCOLCE) (Table 1). Proteins strongly associated with extracellular exosome, extracellular region and extracellular space and membrane-bound organelle in cellular components were distributed throughout the network (Fig. 8 right Suppl. Data File 3).

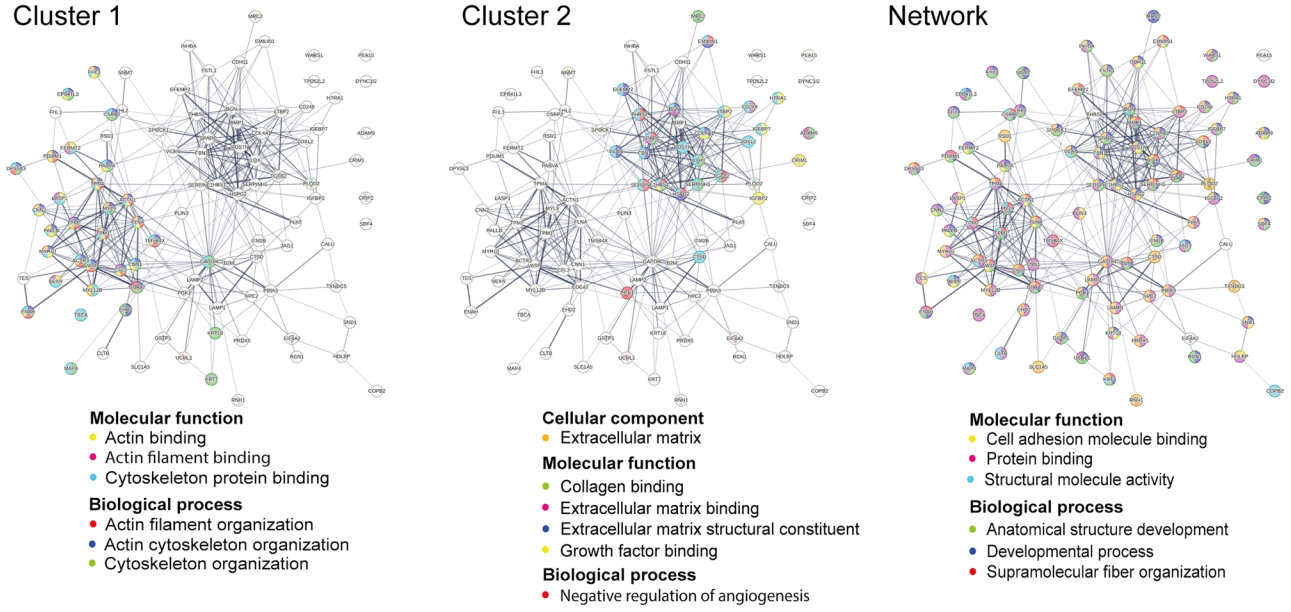

Fig. 7 String analysis and gene ontology analysis of proteins upregulated/ present only in d14-CM. Proteins strongly associated with specific molecular cellular components, molecular functions and biological processes gene ontology terms are shown for two major clusters and network as a whole. Line thickness indicates confidence. Proteins are labeled with the corresponding gene names

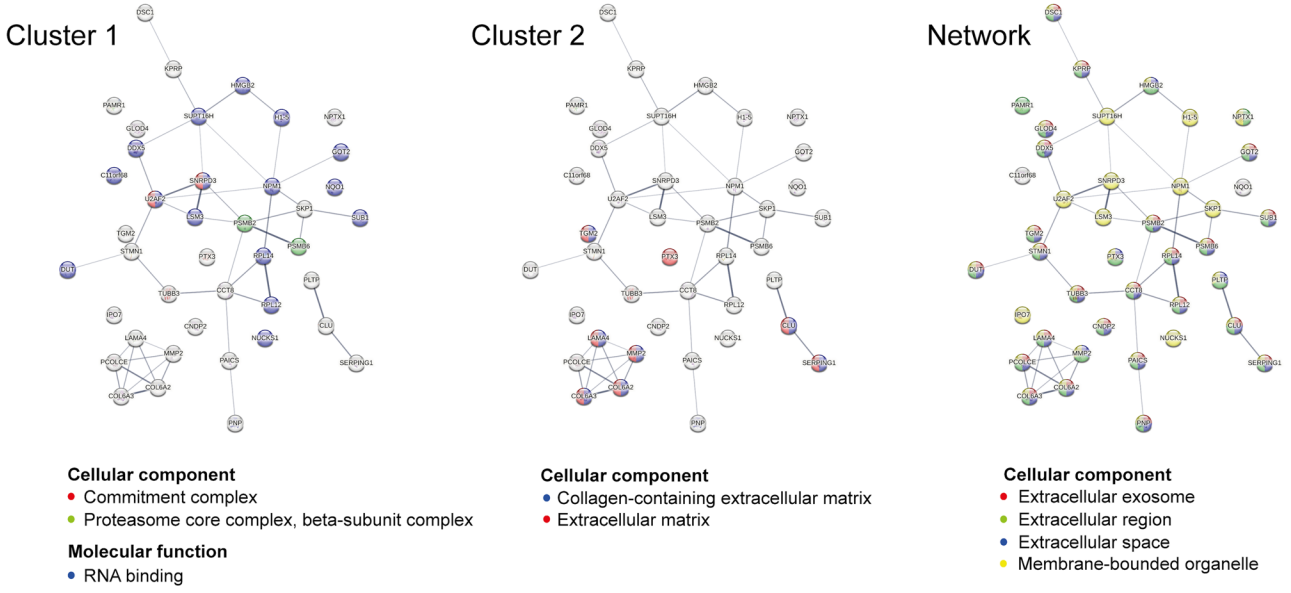

Fig. 8 String analysis and gene ontology analysis of proteins upregulated/ present only in regular CM. Proteins strongly associated with specific molecular cellular components, molecular functions and biological processes gene ontology terms are shown for two major clusters and network as a whole. Line thickness indicates confidence. Proteins are labeled with the corresponding gene names

Overall, our proteomic analyses revealed that proteins functionally associated with actin/cytoskeleton binding and organization, structural components of the cell-extracellular matrix region, and binding to the extracellular matrix are important CM components associated with increased functional activity of hiPSC-MP-derived d14-CM. On the other hand, proteins associated with RNA binding, splicing and the proteasome were downregulated in d14-CM compared to regular CM.

Discussion

Mesenchymal stromal cell secretome represents an attractive, potent alternative to viable cell therapies for bone regeneration. In the current study, we investigated the potential of CM derived from hiPSC-mesenchymal progenitors to induce osteogenic differentiation of adult/aged human bone marrow-derived MSCs. hiPSCs were selected as a promising source of youthful human progenitors that allow scaling up and standardization of

CM production for potential clinical translation. Using a collection of primary bone marrow-derived MSCs from donors aged 20–90 years, we found that hiPSC-MP-CM enhanced early osteogenic differentiation of MSCs from different donors in a dose-dependent manner and to a greater extent than bone marrow-derived MSC-CM. Moreover, prolonged cultivation of hiPSC-MP prior to conditioning enhanced the stimulatory effect of CM, rather than osteogenic predifferentiation. The resulting d14-CM exhibited a distinct, enriched profile of protein components predicted to form a highly interconnected associations network, with protein functions related to actin/cytoskeleton components binding and organization, cell-extracellular matrix region, collagen and growth factor binding, and developmental processes.

One of the major challenges in translating MSC-based therapies into the clinic is the variability of cells between different donors, which affects both the production and efficacy of therapeutic products [62, 63]. Intrinsic cell aging, as well as age-, disease- and risk factor related changes in the tissue and systemic environment may contribute to the decline in regenerative potential of MSCs [29]. Consistent with previous reports, our collection of bone marrow-derived MSCs showed a significant decline in proliferation and trilineage differentiation potential with increasing chronological age of donors [64–66]. However, weak chondrogenic potential was found in several donors over 40 years of age and at least low adipogenic potential in MSCs from all donors, which is consistent with a previous report on MSCs from iliac bone marrow [67]. In contrast, previous studies showed osteogenic differentiation potential and in vitro mineralization of MSCs isolated from femoral bone marrow of donors in a similar age range [68–71], while we did not detect osteogenic differentiation in MSCs from most donors older than 40 years using our standard differentiation model in monolayer culture. As our ethical protocol was limited to information on age and sex of individual donors, no further correlations to donor-related factors could be detected. MSCs from different donors also showed different degrees of senescence, which correlated with their proliferation potential in vitro [72]. The expression of surface antigens was largely consistent with the minimal criteria for defining MSCs [73]. Some deviation was noted for CD146, which has been shown to mark self-renewing clonogenic skeletal progenitors [74], as well as for HLA-DR, which has previously been detected for MSCs after normal culture expansion [75].

The effect of hiPSC-MP-CM on osteogenic differentiation was tested on passage 1 cells, to limit the effects of in vitro culture on cell responses. We observed increased DNA content, indicative of cell proliferation, and increased ALP activity, indicative of early osteogenic differentiation, in MSCs from different donors that otherwise exhibited low differentiation under osteogenic stimulation without CM. These effects of CM exhibited a dose-response profile and required continuous CM delivery, as previously reported [9, 10]. It is noteworthy that ALP activity of MSCs from donors older than 40 years could not be increased to the highest levels observed in the two youngest donors. In contrast, ALP activity of MSCs from these youngest donors was decreased in CM compared to control medium, accompanied by increased DNA content, possibly indicating a shift in osteogenic differentiation kinetics due to increased cell proliferation [76, 77]. In contrast to previous reports [10, 12], we found decreased expression of late osteogenic marker genes and no mineralization in MSC pellets cultured in CM with/without osteogenic supplements. We attribute these results to the lower differentiation potential of MSCs isolated from older human donors compared to MSCs isolated from young rodents under in vitro conditions [10, 12]. Interestingly, in our previous study, culturing bone marrow-derived MSCs from the same donors F71 and M89 on an extracellular matrix derived from the same hiPSC-MPs partially restored the mineralization capacity of the cells, although not to the same extent as in the young donor F20 [35]. It would be interesting to investigate whether the combination of CM components bound to the hiPSC-MP-extracellular matrix could further enhance the activity of aged human bone marrow-derived MSCs.

It is noteworthy that the effect of hiPSC-MP-CM on growth and osteogenic differentiation was higher than that of CM prepared from MSCs from donors M22, F71 and F85. This is consistent with previous studies reporting that the decline in osteogenic capacity of chronologically aged MSCs can be rescued to some extent by exposure to a young extracellular matrix microenvironment [66, 78], and that CM derived from human fetal MSCs can ameliorate replicative senescence of human bone marrow-derived MSCs [79]. Our choice of the hiPSC line was based on our previous study in which MPs derived from this line showed strong growth and trilineage differentiation potential compared to two other lines, an expression profile of surface antigens similar to that of bone marrow-derived MSCs from two donors, and a normal karyotype. In contrast, MPs from another hiPSC line (11c) showed an aberrant profile of surface antigens and a very low trilineage differentiation potential [30]. Screening of cell sources with detailed comparative analyses of CM and cell characterization would be required to clarify the differences between producer cells and the effects of donor age, genetic and epigenetic background of hiPSC lines and/or reprogramming process on secretome components.

Previous studies have shown that MSC cultivation conditions, including serum deprivation [80], hypoxia and

treatment with proinflammatory factors [81–83] and traumatic/degenerative tissue secretome [84] strongly influence the properties of MSC-CM. With the aim of improving osteogenic differentiation of MSCs, we tested whether osteogenic pre-differentiation of hiPSC-MPs or prolonged cultivation could further enhance their CM activity. To the best of our knowledge, our study is the first to show a strong effect of prolonged cultivation of MSC-like progenitor cells on the potential of their CM to stimulate osteogenic differentiation. We found that increased levels of TGFβ–1, previously identified as one of the major bone regenerative components in the CM of MSCs [11, 12], corresponded with increased CM stimulatory activity. Furthermore, we detected a distinct, enriched profile of protein components in d14-CM compared to regular CM. Together with proteins unique to d14-CM, the upregulated proteins formed a more complex and more interconnected String network of functional associations than the proteins that were upregulated/unique in regular CM.

Several of the most upregulated proteins in d14-CM appeared as hubs with multiple connections in the String network for functional associations. Within cluster 2, which was functionally associated with ECM structural constituents and with collagen, growth factor and ECM binding, several upregulated hub proteins were identified. The most upregulated was perlecan, a multifunctional, cell-instructive, matrix-stabilizing proteoglycan previously shown to promote embryonic cell proliferation, differentiation and tissue development, as well as connective tissue repair and angiogenesis through interaction with VEGF, PDGF, FGF and BMP [42]. Interestingly, perlecan-based peptides and recombinant domains have already been used in tissue engineering studies to induce cell differentiation and deliver growth factors [42]. IGFBP7, another highly upregulated hub protein, has been shown to regulate osteogenic differentiation of human bone marrow-derived MSCs via the Wnt/β-catenin signaling pathway [44] and has been used to convert human fibroblasts into osteoblasts [85]. Other upregulated hub proteins in cluster 2 included LOXL2, which has previously been investigated to increase collagen cross-linking in tissue engineered osteogenic grafts [86]; thrombospondin 2, which has been shown to influence cartilage-to-bone ratio and vascularization during fracture healing [47, 48]; and versican, a large chondroitin sulfate proteoglycan that plays a central role in tissue morphogenesis and maintenance by regulating TGFβ and BMP signaling [51]. Interestingly, the regulation of growth factor signaling by versican has been suggested to occur via the binding of fibrillin and latent TGFβ binding proteins [51], and fibrillin-1 was also one of the upregulated hub proteins identified in d14-CM. SPARC, which is involved in ECM synthesis, cell adhesion and spreading, collagen calcification and maintenance of bone mass [52], PDIA3, which has been shown to promote a matrix-rich secretome via association with thrombospondin 1 and to stimulate fibroblast adhesion [50], biglycan, a member of the family of small leucine-rich proteoglycans shown to regulate bone development and regeneration [53], IGFBP2, whose signaling has been shown to trigger osteogenic differentiation of dexamethasone-treated human bone marrow-derived MSCs in cross talk with integrin alpha 5 [56], periostin, a structural component of bone matrix and a signaling molecule that stimulates bone formation [87] and growth factors BMP–1 and TGFβ–2 were also among the upregulated or uniquely identified proteins in cluster 2 of d14-CM network of functional associations. Periostin and BMP–1 have been shown to promote proteolytic activation of lysyl oxidase, another unique protein of d14-CM, which catalyzes cross-linking between collagen fibrils and determines the mechanical properties of connective tissues [88]. Identified growth factors TGFβ–1, TGFβ–2 and BMP–1 belong to the TGF-β superfamily and exert essential functions during osteoblast and chondrocyte lineage commitment and differentiation, skeletal development, and homeostasis [89].

On the other hand, LASP1 was an upregulated protein hub in cluster 1 of the d14-CM network that was functionally associated with the binding and organization of actin/cytoskeletal components. LASP1 was first demonstrated in mammary and other cancer cells, and it was only recently reported that it plays a role in embryonic development in the zebrafish model [43]. Several other cytoskeleton-associated proteins have been identified in cluster 1, including tropomyosin 1, -2 and −3, myosin light and heavy chain proteins and filamin A, which cross-links actin filaments, links actin filaments to membrane glycoproteins and is involved in cytoskeletal remodeling to induce changes in cell shape and migration [90]. Recently, filamin A has also been shown to be an important regulator of bone formation and resorption processes [91]. Overall, our analyses of d14-CM protein components indicate the importance of the extracellular matrix in interacting with MSCs and influencing cell shape and proliferation in the early stages of osteogenic differentiation, as well as for the sequestration of growth factors involved in bone regeneration. Previous studies have shown that not only soluble signals but also cell shape and cytoskeletal tension regulate osteogenic commitment of MSCs via Rho signaling [92, 93], and new biomaterials with suitable micro- and nanotopography are currently being investigated to enable biomechanical stimulation during bone regeneration [94].

In contrast, the proteins that were upregulated in regular CM were mostly associated with RNA binding, splicing and the proteasome (cluster 1) and with the

extracellular collagen matrix and extracellular matrix components (cluster 2) (Table 1). Nucleophosmin 1 and stathmin 1, both of which play essential roles in the regulation of cell proliferation, were the most upregulated [57, 58]. Nucleophosmin is ubiquitously expressed in human cells, and stathmin 1 has been detected in human and rat osteoblast-like cells [95] and in growth plate chondrocytes [96]. Other upregulated components included the ribosomal component RPL12 [59], pentraxin 3, which has been shown to induce osteogenic differentiation in an inflammatory environment [60], and the procollagen C endopeptidase enhancer (PCOLCE), which mediates enzymatic cleavage of type I procollagen [61]. Overall, our analysis of regular CM suggests the presence of unique/upregulated components involved in protein metabolism and regulation of cell proliferation, in addition to components with functional connections in the extracellular matrix identified in both regular CM and d14-CM.

Previous studies have identified components associated with extracellular region, extracellular exosomes, extracellular matrix interaction, cell adhesion and cytoskeleton in CM preparations of MSCs from the amnion [97], adipose tissue, placenta, Wharton's jelly and bone marrow [83, 98], as well as in hiPSC-, human embryonic stem cell- and human umbilical cord MSC-derived exosomes [99]. However, the potential of these CM/exosome preparations to enhance osteogenic differentiation has not been investigated. On the other hand, various growth factors and cytokines were identified as major components of unfractionated MSC-CM that promoted bone regeneration in animal models [8–12]. Our results complement these studies by showing that the enhanced stimulation of osteogenic differentiation of bone marrow-derived MSC by d14-CM is associated with a network of protein components functionally involved in cell cytoskeleton assembly, extracellular matrix components, and cell-extracellular matrix interactions. Our data thus provide insight into the "amplified" profile of d14-CM of hiPSC-MPs, which could be further modulated by optimizing cell cultivation parameters, including media composition, oxygen level, senescence induction, biochemical/biophysical stimulation, and culture dimensionality [100].

It is also important to note that our proteomic analysis included unfractionated CM preparations, while previous studies showed specific effects mediated by the EV fraction of CM [19, 21, 23]. In our ongoing studies, we are investigating the effects of MSC source, chronological age, and culture conditions on the release profile and cargo of EVs contained in MSC-CM. Given our current data, it is likely that further development of bone regenerative therapies based on CM will require not only the identification and combination of a few key "active" components in CM, but also the identification of complex protein signaling networks that work together to achieve the best functional outcomes in promoting bone regeneration processes. It is likely that using CM preparations (or their separated and concentrated soluble or vesicular components) will present an advantage for bone regeneration over delivery of single identified secretome components.

The current study has several limitations. First, it was designed as a proof of concept and therefore only a single hiPSC line was used for the preparation of CM. Our choice of the hiPSC line was based on our previous study in which MPs derived from this line showed a strong differentiation potential compared to MPs from two other hiPSC lines, as well as a surface antigen expression profile similar to that of primary bone marrow-derived MSCs from two donors [30]. However, it is likely that screening of other hiPSC lines (with different genetic/epigenetic background) could yield MPs and secretomes with further improved regenerative properties. We propose that the protein networks identified in the current study would be useful in such screening/optimization studies. Second, osteogenic responses were tested using standard MSC differentiation models in monolayer and pellet cultures. In order to evaluate the responses of mature osteoblastic cells, MSC pre-differentiation would be required. Furthermore, testing of optimized CM preparations using in vivo models with well-considered dosing regimens and delivery approaches will be key to confirm their bone regenerative potential.

Conclusions

In conclusion, our data show that hiPSC-MP-CM enhances early osteogenic differentiation of adult/aged human bone marrow-derived MSCs, and this effect was stronger than that observed with bone marrow-derived MSC CM. Importantly, prolonged cultivation of hiPSC-MP rather than osteogenic pre-differentiation strongly increased the stimulatory effect of CM. Proteomic analysis revealed a distinct, more complex protein profile in d14-CM, and the identified proteins formed a highly interconnected network of functional associations with roles in binding and organization of the actin/cytoskeleton, structural components of the cell-extracellular matrix region, and binding to the extracellular matrix. On the other hand, proteins functionally associated with RNA binding, splicing and the proteasome as well as with the extracellular matrix were upregulated in regular CM. Taken together, our analyses provide the basis for further optimization of hiPSC-MP-CM for bone regenerative therapies and demonstrate the importance of evaluating protein interaction networks to optimize the functional potential of CM for regenerative treatments.

Abbreviations

CM	Conditioned medium
CTRL	Control medium
d14-CM	Conditioned medium after 14 days in growth medium
d14OST-CM	Conditioned medium after 14 days in osteogenic medium
Evs	Extracellular vesicles
hiPSCs	Human induced pluripotent stem cells
hiPSC-MPs	Hipsc-mesenchymal progenitors
MSCs	Mesenchymal stromal cells

Supplementary Information

The online version contains supplementary material available at https://doi.org/10.1186/s13287-024-03960-5.

Supplementary Material 1

Supplementary Material 2

Supplementary Material 3

Supplementary Material 4

Supplementary Material 5

Supplementary Material 6

Supplementary Material 7

Supplementary Material 8

Acknowledgements

We thank the personnel of the Lorenz-Böhler-Unfallkrankenhaus for providing the human tissue waste for primary cell isolation and the New York Stem Cell Foundation Research Institute for providing the human induced pluripotent stem cell line 1013 A and its mesenchymal progenitors. We also thank all our colleagues at the Ludwig Boltzmann Institute for Traumatology for their suggestions and ongoing support of the project. InstaText writing tool (https://instatext.io) was used to edit the English language of the final manuscript.

Author contributions

DMP and HR conceptualized and designed the study. VG, LO, DH, ALS, AT, LP, JO, and JZ isolated, cultivated, and characterized human bone marrow-derived MSCs and prepared conditioned media. VG, LO, DH and BS tested and analysed the effects of conditioned media on bone marrow-derived MSCs' proliferation and osteogenic differentiation. DMP, DH, BB and GM perfomed proteomic and statistical analyses. DMP, VG, LO, DH, JO, WH, JG and HR reviewed collected data and suggested improvements to the study. DMP prepared the manuscript draft. All authors reviewed and edited the manuscript, were informed about each step of processing and have read and approved the final manuscript.

Funding

This work has received funding from the European Union's Horizon 2020 research and innovation program under the Marie Sklodowska-Curie actions (grant agreement No. 657716) and the Transforming European Industry call H2020-NMBP-TRIND-2020 (grant agreement No. 953134), as well as by the FFG Industrienahe Dissertation program (grant agreement No. 867803 and 853056), the FEMtech Praktika program (grant agreement No. 852154, 868917 and 877951) and the Production of the Future program (grant agreement No. 877452).

Data availability

All data generated and analysed during this study are included in this published article and its supplementary information files. The mass spectrometry proteomics data have been deposited to the ProteomeXchange Consortium via the PRIDE partner repository with the dataset identifier PXD052766 (access details are provided in Suppl. Data File 1). The raw datasets used and/or analysed during the current study are available from the corresponding author on reasonable request.

Declarations

Ethics approval and consent to participate

The study was conducted with informed consent for the research use of tissue remaining after surgery and with full ethical approval by the Ethics Committee for the AUVA Hospitals ("Ethikkomission der AUVA", Vienna, Austria)", approval No. 1/2005, title "Tracking and improving cartilage regeneration in a human cartilage defect in vivo model" ("Vervolgung und Verbesserung der Knorpelregeneration in einem humanen Knorpeldefekt in vivo Modell"), approved February 9th 2006, and amendment from September 28th 2009, to include "The extraction of demineralized bone, analytical determinations in the spongiosa area, and isolation of osteoblasts and bone marrow" ("Die Gewinnung von demineralisiertem Knochen, Analytische Bestimmungen im Spongiosabereich, isolierung von Osteoblasten und Knochenmark"). The patients provided written informed consent for the use of samples.

Consent for publication

All authors confirm their consent for publication.

Competing interests

Authors of the study declare no competing interests.

Author details

[1]Ludwig Boltzmann Institute for Traumatology, The Research Centre in Cooperation with AUVA, Donaueschingenstrasse 13, Vienna A-1200, Austria
[2]Austrian Cluster for Tissue Regeneration, Donaueschingenstrasse 13, Vienna 1200, Austria
[3]Institute of Science and Technology Austria, Am Campus 1, Klosterneuburg 3400, Austria
[4]Clinical Department of Laboratory Medicine Proteomics Core Facility, Medical University of Vienna, Spitalgasse 23, Vienna 1090, Austria
[5]Bruker Austria, Lemböckgasse 47b, Vienna 1230, Austria
[6]University Clinic of Dentistry, Medical University of Vienna, Sensengasse 2a, Vienna 1090, Austria
[7]Department of Biotechnology, BOKU - University of Natural Resources and Life Sciences Vienna, Gregor-Mendel-Straße 33, Vienna 1180, Austria

Received: 5 June 2024 / Accepted: 25 September 2024
Published online: 17 November 2024

References

1. Marolt Presen D, Traweger A, Gimona M, Redl H. Mesenchymal stromal cell-based bone regeneration therapies: from cell transplantation and tissue Engineering to Therapeutic Secretomes and Extracellular vesicles. Front Bioeng Biotechnol. 2019;7:352.
2. Giannoni P, Scaglione S, Daga A, Ilengo C, Cilli M, Quarto R. Short-time survival and engraftment of bone marrow stromal cells in an ectopic model of bone regeneration. In: Tissue Engineering - Part A. 2010. pp. 489–99.
3. Becquart P, Cambon-Binder A, Monfoulet LE, Bourguignon M, Vandamme K, Bensidhoum M, et al. Ischemia is the prime but not the only cause of human multipotent stromal cell death in tissue-engineered constructs in vivo. Tissue Eng - Part A. 2012;18(19–20):2084–94.
4. Manassero M, Paquet J, Deschepper M, Viateau V, Retortillo J, Bensidhoum M et al. Comparison of Survival and Osteogenic Ability of Human Mesenchymal Stem Cells in Orthotopic and Ectopic Sites in Mice. Tissue Eng - Part A [Internet]. 2016;22(5–6):534–44. http://online.liebertpub.com/doi/https://doi.org/10.1089/ten.tea.2015.0346
5. Caplan AI, Dennis JE. Mesenchymal stem cells as trophic mediators. J Cell Biochem. 2006;98:1076–84.
6. Hofer HR, Tuan RS. Secreted trophic factors of mesenchymal stem cells support neurovascular and musculoskeletal therapies. 7, Stem Cell Research and Therapy. 2016. p. 131.
7. Gimona M, Pachler K, Laner-Plamberger S, Schallmoser K, Rohde E. Manufacturing of human extracellular vesicle-based therapeutics for clinical use. Int J Mol Sci. 2017;18(6):E1190.
8. Osugi M, Katagiri W, Yoshimi R, Inukai T, Hibi H, Ueda M. Conditioned media from mesenchymal stem cells enhanced bone regeneration in rat calvarial bone defects. Tissue Eng - Part A. 2012;18(13–14):1479–89.

9. Ando Y, Matsubara K, Ishikawa J, Fujio M, Shohara R, Hibi H, et al. Stem cell-conditioned medium accelerates distraction osteogenesis through multiple regenerative mechanisms. Bone. 2014;61:82–90.
10. Ogata K, Katagiri W, Osugi M, Kawai T, Sugimura Y, Hibi H, et al. Evaluation of the therapeutic effects of conditioned media from mesenchymal stem cells in a rat bisphosphonate-related osteonecrosis of the jaw-like model. Bone. 2015;74:95–105.
11. Katagiri W, Kawai T, Osugi M, Sugimura-Wakayama Y, Sakaguchi K, Kojima T, et al. Angiogenesis in newly regenerated bone by secretomes of human mesenchymal stem cells. Maxillofac Plast Reconstr Surg. 2017;39(1):8.
12. Katagiri W, Sakaguchi K, Kawai T, Wakayama Y, Osugi M, Hibi H. A defined mix of cytokines mimics conditioned medium from cultures of bone marrow-derived mesenchymal stem cells and elicits bone regeneration. Cell Prolif. 2017;50(3).
13. Ogata K, Matsumura M, Moriyama M, Katagiri W, Hibi H, Nakamura S. Cytokine mixtures mimicking secretomes from mesenchymal stem cells improve medication-related osteonecrosis of the Jaw in a rat model. JBMR Plus. 2018;2(2):69–80.
14. Furuta T, Miyaki S, Ishitobi H, Ogura T, Kato Y, Kamei N, et al. Mesenchymal stem cell-derived Exosomes Promote Fracture Healing in a mouse model. Stem Cells Transl Med. 2016;5(12):1620–30.
15. Diomede F, Gugliandolo A, Cardelli P, Merciaro I, Ettorre V, Traini T, et al. Three-dimensional printed PLA scaffold and human gingival stem cell-derived extracellular vesicles: a new tool for bone defect repair. Stem Cell Res Ther. 2018;9(1):104.
16. Lu Z, Chen Y, Dunstan C, Roohani-Esfahani S, Zreiqat H. Priming adipose stem cells with Tumor Necrosis factor-alpha Preconditioning Potentiates their exosome efficacy for bone regeneration. Tissue Eng - Part A. 2017;23(21–22):1212–20.
17. Narayanan R, Huang CC, Ravindran S. Hijacking the Cellular Mail: Exosome mediated differentiation of mesenchymal stem cells. Stem Cells Int. 2016;2016:3808674.
18. Li W, Liu Y, Zhang P, Tang Y, Zhou M, Jiang W, et al. Tissue-Engineered Bone immobilized with human adipose stem cells-derived Exosomes promotes bone regeneration. ACS Appl Mater Interfaces. 2018;10(6):5240–54.
19. Qi X, Zhang J, Yuan H, Xu Z, Li Q, Niu X, et al. Exosomes secreted by human-induced pluripotent stem cell-derived mesenchymal stem cells repair critical-sized bone defects through enhanced angiogenesis and osteogenesis in osteoporotic rats. Int J Biol Sci. 2016;12(7):836–49.
20. Zhang J, Liu X, Li H, Chen C, Hu B, Niu X, et al. Exosomes/tricalcium phosphate combination scaffolds can enhance bone regeneration by activating the PI3K/Akt signaling pathway. Stem Cell Res Ther. 2016;7(1):136.
21. Qin Y, Wang L, Gao Z, Chen G, Zhang C. Bone marrow stromal/stem cell-derived extracellular vesicles regulate osteoblast activity and differentiation in vitro and promote bone regeneration in vivo. Sci Rep. 2016;6:21961.
22. Zhang L, Jiao G, Ren S, Zhang X, Li C, Wu W et al. Exosomes from bone marrow mesenchymal stem cells enhance fracture healing through the promotion of osteogenesis and angiogenesis in a rat model of nonunion. Stem Cell Res Ther. 2020;11(1).
23. Zhang Y, Hao Z, Wang P, Xia Y, Wu J, Xia D, et al. Exosomes from human umbilical cord mesenchymal stem cells enhance fracture healing through HIF-1α-mediated promotion of angiogenesis in a rat model of stabilized fracture. Cell Prolif. 2019;52(2):e12570.
24. Borrelli J, Pape C, Hak D, Hsu J, Lin S, Giannoudis P, et al. Physiological challenges of bone repair. J Orthop Trauma. 2012;26(12):708–11.
25. Gruber R, Koch H, Doll BA, Tegtmeier F, Einhorn TA, Hollinger JO. Fracture healing in the elderly patient. 41, Experimental Gerontology. 2006;41(11):1080–93. https://doi.org/10.1016/j.exger.2006.09.008
26. Weilner S, Schraml E, Wieser M, Messner P, Schneider K, Wassermann K, et al. Secreted microvesicular miR-31 inhibits osteogenic differentiation of mesenchymal stem cells. Aging Cell. 2016;15(4):744–54.
27. Weilner S, Keider V, Winter M, Harreither E, Salzer B, Weiss F, et al. Vesicular Galectin-3 levels decrease with donor age and contribute to the reduced osteo-inductive potential of human plasma derived extracellular vesicles. Aging. 2016;8(1):16–33.
28. Davis C, Dukes A, Drewry M, Helwa I, Johnson MH, Isales CM, et al. MicroRNA-183-5p increases with age in bone-derived extracellular vesicles, suppresses bone marrow stromal (stem) cell proliferation, and induces stem cell senescence. Tissue Eng - Part A. 2017;23(21–22):1231–40.
29. Baker N, Boyette LB, Tuan RS. Characterization of bone marrow-derived mesenchymal stem cells in aging. Bone. 2015;70:37–47.
30. De Peppo GM, Marcos-Campos I, Kahler DJ, Alsalman D, Shang L, Vunjak-Novakovic G, et al. Engineering bone tissue substitutes from human induced pluripotent stem cells. Proc Natl Acad Sci U S A. 2013;110(21):8680–5.
31. Frobel J, Hemeda H, Lenz M, Abagnale G, Joussen S, Denecke B, et al. Epigenetic rejuvenation of mesenchymal stromal cells derived from induced pluripotent stem cells. Stem Cell Rep. 2014;3(3):414–22.
32. Katagiri W, Osugi M, Kawai T, Ueda M. Novel cell-free regeneration of bone using stem cell–derived growth factors. Int J Oral Maxillofac Implants. 2013;28(4):1009–16.
33. Marolt D, Rode M, Kregar-Velikonja N, Jeras M, Knezevic M. Primary human alveolar bone cells isolated from tissue samples acquired at periodontal surgeries exhibit sustained proliferation and retain osteogenic phenotype during in vitro expansion. PLoS ONE. 2014;9(3).
34. Marolt D, Augst A, Freed LE, Vepari C, Fajardo R, Patel N, et al. Bone and cartilage tissue constructs grown using human bone marrow stromal cells, silk scaffolds and rotating bioreactors. Biomaterials. 2006;27(36):6138–49.
35. Hanetseder D, Levstek T, Teuschl-Woller AH, Frank JK, Schaedl B, Redl H et al. Engineering of extracellular matrix from human iPSC-mesenchymal progenitors to enhance osteogenic capacity of human bone marrow stromal cells independent of their age. Front Bioeng Biotechnol. 2023;11.
36. Xu S, Evans H, Buckle C, De Veirman K, Hu J, Xu D, et al. Impaired osteogenic differentiation of mesenchymal stem cells derived from multiple myeloma patients is associated with a blockade in the deactivation of the notch signaling pathway. Leukemia. 2012;26:2546–9.
37. Kong AT, Leprevost FV, Avtonomov DM, Mellacheruvu D, Nesvizhskii AI, MSFragger. Ultrafast and comprehensive peptide identification in mass spectrometry-based proteomics. Nat Methods. 2017;14(5).
38. Tyanova S, Temu T, Sinitcyn P, Carlson A, Hein MY, Geiger T et al. The Perseus computational platform for comprehensive analysis of (prote)omics data. 13, Nat Methods. 2016.
39. Szklarczyk D, Gable AL, Lyon D, Junge A, Wyder S, Huerta-Cepas J, et al. STRING v11: protein-protein association networks with increased coverage, supporting functional discovery in genome-wide experimental datasets. Nucleic Acids Res. 2019;47:D1.
40. Deutsch EW, Bandeira N, Perez-Riverol Y, Sharma V, Carver JJ, Mendoza L, et al. The ProteomeXchange consortium at 10 years: 2023 update. Nucleic Acids Res. 2023;51:D1.
41. Perez-Riverol Y, Bai J, Bandla C, García-Seisdedos D, Hewapathirana S, Kamatchinathan S, et al. The PRIDE database resources in 2022: a hub for mass spectrometry-based proteomics evidences. Nucleic Acids Res. 2022;50:D1.
42. Hayes AJ, Farrugia BL, Biose IJ, Bix GJ, Melrose J. Perlecan, A Multi-Functional. Cell-Instructive, matrix-stabilizing Proteoglycan with roles in tissue development has relevance to connective tissue repair and regeneration. Vol. 10, Frontiers in Cell and Developmental Biology. 2022.
43. Grossi I, Schiavone M, Cannone E, Grejdan OA, Tobia C, Bonomini F et al. Lasp1 expression is implicated in embryonic development of zebrafish. Genes (Basel). 2023;14(1).
44. Zhang W, Chen E, Chen M, Ye C, Qi Y, Ding Q et al. IGFBP7 regulates the osteogenic differentiation of bone marrow-derived mesenchymal stem cells via Wnt/β-catenin signaling pathway. FASEB J. 2018;32(4).
45. Mitra D, Yasui OW, Harvestine JN, Link JM, Hu JC, Athanasiou KA et al. Exogenous Lysyl Oxidase-Like 2 and Perfusion Culture Induce Collagen Crosslink formation in osteogenic grafts. Biotechnol J. 2019;14(3).
46. Zumbrunn J, Trueb B. Primary structure of a putative serine protease specific for IGF-binding proteins. FEBS Lett. 1996;398:2–3.
47. Taylor DK, Meganck JA, Terkhorn S, Rajani R, Naik A, O'Keefe RJ et al. Thrombospondin-2 influences the proportion of cartilage and bone during fracture healing. J Bone Min Res. 2009;24(6).
48. Miedel E, Dishowitz MI, Myers MH, Dopkin D, Yu YY, Miclau TS et al. Disruption of thrombospondin-2 accelerates ischemic fracture healing. J Orthop Res. 2013;31(6).
49. Robinson PJ, Pringle MA, Fleming B, Bulleid NJ. Distinct role of ERp57 and ERdj5 as a disulfide isomerase and reductase during ER protein folding. J Cell Sci. 2023;136(2).
50. Hellewell AL, Heesom KJ, Jepson MA, Adams JC. PDIA3/ERp57 promotes a matrix-rich secretome that stimulates fibroblast adhesion through CCN2. Am J Physiol - Cell Physiol. 2022;322(4).
51. Watanabe H. Aggrecan and versican: two brothers close or apart. Volume 322. American Journal of Physiology - Cell Physiology; 2022.

52. Rosset EM, Bradshaw AD. SPARC/osteonectin in mineralized tissue. Vols. 52–54, Matrix Biology. 2016.
53. Shainer R, Kram V, Kilts TM, Li L, Doyle AD, Shainer I et al. Biglycan regulates bone development and regeneration. Front Physiol. 2023;14.
54. Kitahama S, Gibson MA, Hatzinikolas G, Hay S, Kuliwaba JL, Evdokiou A et al. Expression of fibrillins and other microfibril-associated proteins in human bone and osteoblast-like cells. Bone. 2000;27(1).
55. Conover CA. Insulin-like growth factor-binding proteins and bone metabolism. Volume 294. American Journal of Physiology - Endocrinology and Metabolism; 2008.
56. Hamidouche Z, Fromigué O, Ringe J, Häupl T, Marie PJ. Crosstalks between integrin alpha 5 and IGF2/IGFBP2 signalling trigger human bone marrow-derived mesenchymal stromal osteogenic differentiation. BMC Cell Biol. 2010;11.
57. Patel SS, Kluk MJ, Weinberg OK. NPM1 Biology in Myeloid Neoplasia. Volume 15. Current Hematologic Malignancy Reports; 2020.
58. Belletti B, Baldassarre G, Stathmin. A protein with many tasks. New biomarker and potential target in cancer. Volume 15. Expert Opinion on Therapeutic Targets; 2011.
59. Chu W, Presky DH, Swerlick RA, Burns DK. The primary structure of human ribosomal protein L12. Volume 21. Nucleic Acids Research; 1993.
60. Dong W, Xu X, Luo Y, Yang C, He Y, Dong X et al. PTX3 promotes osteogenic differentiation by triggering HA/CD44/FAK/AKT positive feedback loop in an inflammatory environment. Bone. 2022;154.
61. Vadon-Le Goff S, Kronenberg D, Bourhis JM, Bijakowski C, Raynal N, Ruggiero F et al. Procollagen C-proteinase enhancer stimulates procollagen processing by binding to the C-propeptide region only. J Biol Chem. 2011;286(45).
62. Zha K, Li X, Yang Z, Tian G, Sun Z, Sui X, et al. Heterogeneity of mesenchymal stem cells in cartilage regeneration: from characterization to application. Volume 6. npj Regenerative Medicine; 2021.
63. Levy O, Kuai R, Siren EMJ, Bhere D, Milton Y, Nissar N, et al. Shattering barriers toward clinically meaningful MSC therapies. Sci Adv. 2020;6:30.
64. Stolzing A, Jones E, McGonagle D, Scutt A. Age-related changes in human bone marrow-derived mesenchymal stem cells: consequences for cell therapies. Mech Ageing Dev. 2008;129(3):163–73.
65. Churchman SM, Boxall SA, McGonagle D, Jones EA. Predicting the remaining Lifespan and Cultivation-related loss of osteogenic capacity of bone marrow multipotential stromal cells Applicable across a broad Donor Age Range. Stem Cells Int. 2017;2017:6129596.
66. Carvalho MS, Alves L, Bogalho I, Cabral JMS, da Silva CL. Impact of Donor Age on the osteogenic supportive capacity of mesenchymal stromal cell-derived Extracellular Matrix. Front Cell Dev Biol. 2021;9.
67. Kanawa M, Igarashi A, Ronald VS, Higashi Y, Kurihara H, Sugiyama M et al. Age-dependent decrease in the chondrogenic potential of human bone marrow mesenchymal stromal cells expanded with fibroblast growth factor-2. Cytotherapy. 2013;15(9).
68. Nguyen VT, Tessaro I, Marmotti A, Sirtori C, Peretti GM, Mangiavini L. Does the harvesting site influence the osteogenic potential of mesenchymal stem cells? Stem Cells Int. 2019;2019.
69. Wagenbrenner M, Heinz T, Horas K, Jakuscheit A, Arnholdt J, Herrmann M et al. The human arthritic hip joint is a source of mesenchymal stromal cells (MSCs) with extensive multipotent differentiation potential. BMC Musculoskelet Disord. 2020;21(1).
70. Kern S, Eichler H, Stoeve J, Klüter H, Bieback K. Comparative analysis of mesenchymal stem cells from bone marrow, umbilical cord blood, or adipose tissue. Stem Cells. 2006;24(5):1294–301.
71. Herrmann M, Hildebrand M, Menzel U, Fahy N, Alini M, Lang S, et al. Phenotypic characterization of bone marrow mononuclear cells and derived stromal cell populations from human Iliac Crest, vertebral body and femoral head. Int J Mol Sci. 2019;20(14):3454.
72. Stenderup K, Justesen J, Clausen C, Kassem M. Aging is associated with decreased maximal life span and accelerated senescence of bone marrow stromal cells. Bone. 2003;33(6).
73. Dominici M, Le Blanc K, Mueller I, Slaper-Cortenbach I, Marini FC, Krause DS et al. Minimal criteria for defining multipotent mesenchymal stromal cells. The International Society for Cellular Therapy position statement. Cytotherapy [Internet]. 2006;8(4):315–7. http://www.sciencedirect.com/science/article/pii/S1465324906708817
74. Sacchetti B, Funari A, Michienzi S, Di Cesare S, Piersanti S, Saggio I, et al. Self-renewing osteoprogenitors in bone marrow sinusoids can organize a hematopoietic microenvironment. Cell. 2007;131(2):324–36.
75. Grau-Vorster M, Laitinen A, Nystedt J, Vives J. HLA-DR expression in clinical-grade bone marrow-derived multipotent mesenchymal stromal cells: a two-site study. Stem Cell Res Ther. 2019;10(1).
76. Malaval L, Modrowski D, Gupta AK, Aubin JE. Cellular expression of bone-related proteins during in vitro osteogenesis in rat bone marrow stromal cell cultures. J Cell Physiol. 1994;158(3).
77. Quarles LD, Yohay DA, Lever LW, Caton R, Wenstrup RJ. Distinct proliferative and differentiated stages of murine MC3T3-E1 cells in culture: an in vitro model of osteoblast development. J Bone Min Res. 1992;7(6).
78. Sun Y, Li W, Lu Z, Chen R, Ling J, Ran Q, et al. Rescuing replication and osteogenesis of aged mesenchymal stem cells by exposure to a young extracellular matrix. FASEB J. 2011;25(5):1474–85.
79. Wang B, Lee WYW, Huang B, Zhang JF, Wu TY, Jiang X, et al. Secretome of human fetal mesenchymal stem cell ameliorates replicative senescen. Stem Cells Dev. 2016;25(22):1755–66.
80. Oskowitz A, McFerrin H, Gutschow M, Carter ML, Pochampally R. Serum-deprived human multipotent mesenchymal stromal cells (MSCs) are highly angiogenic. Stem Cell Res. 2011;6(3):215–25.
81. Ferreira JR, Teixeira GQ, Santos SG, Barbosa MA, Almeida-Porada G, Gonçalves RM. Mesenchymal stromal cell secretome: influencing therapeutic potential by cellular pre-conditioning. 9, Frontiers in Immunology. 2018.
82. Ragni E, Perucca Orfei C, De Luca P, Mondadori C, Viganò M, Colombini A et al. Inflammatory priming enhances mesenchymal stromal cell secretome potential as a clinical product for regenerative medicine approaches through secreted factors and EV-miRNAs: The example of joint disease. Stem Cell Res Ther. 2020;11(1).
83. Maffioli E, Nonnis S, Angioni R, Santagata F, Calì B, Zanotti L et al. Proteomic analysis of the secretome of human bone marrow-derived mesenchymal stem cells primed by pro-inflammatory cytokines. J Proteom. 2017;166.
84. Wangler S, Kamali A, Wapp C, Wuertz-Kozak K, Häckel S, Fortes C et al. Uncovering the secretome of mesenchymal stromal cells exposed to healthy, traumatic, and degenerative intervertebral discs: a proteomic analysis. Stem Cell Res Ther. 2021;12(1).
85. Lu ZF, Chiu J, Lee LR, Schindeler A, Jackson M, Ramaswamy Y et al. Reprogramming of human fibroblasts into osteoblasts by insulin-like growth factor-binding protein 7. Stem Cells Transl Med. 2020;9(3).
86. Mitra D, Whitehead J, Yasui OW, Leach JK. Bioreactor culture duration of engineered constructs influences bone formation by mesenchymal stem cells. Biomaterials. 2017;146:29–39.
87. Bonnet N, Garnero P, Ferrari S. Periostin action in bone. Mol Cell Endocrinol 2016;432.
88. Maruhashi T, Kii I, Saito M, Kudo A. Interaction between periostin and BMP-1 promotes proteolytic activation of lysyl oxidase. J Biol Chem. 2010;285(17).
89. Wu M, Wu S, Chen W, Li YP. The roles and regulatory mechanisms of TGF-β and BMP signaling in bone and cartilage development, homeostasis and disease. 34, Cell Res. 2024.
90. Lamsoul I, Dupré L, Lutz PG. Molecular tuning of Filamin A activities in the Context of Adhesion and Migration. 8, Frontiers in Cell and Developmental Biology. 2020.
91. Yang C, Yang P, Liu P, Wang H, Ke E, Li K et al. Targeting Filamin A alleviates ovariectomy-induced bone loss in mice via the WNT/β-catenin signaling pathway. Cell Signal. 2022;90.
92. McBeath R, Pirone DM, Nelson CM, Bhadriraju K, Chen CS. Cell shape, cytoskeletal tension, and RhoA regulate stem cell lineage commitment. Dev Cell. 2004;6(4).
93. Kamioka H, Sugawara Y, Honjo T, Yamashiro T, Takano-Yamamoto T. Terminal differentiation of osteoblasts to osteocytes is accompanied by dramatic changes in the distribution of actin-binding proteins. J Bone Min Res. 2004;19(3).
94. Melo-Fonseca F, Miranda G, Domingues HS, Pinto IM, Gasik M, Silva FS. Reengineering Bone-Implant interfaces for Improved Mechanotransduction and Clinical outcomes. Volume 16. Stem Cell Reviews and Reports; 2020.
95. Kumar R, Haugen JD. Human and rat osteoblast-like cells express stathmin, a growth-regulatory protein. Biochem Biophys Res Commun. 1994;201(2).
96. Hummert TW, Schwartz Z, Sylvia VL, Dean DD, Hardin RR, Boyan BD. Expression and production of stathmin in growth plate chondrocytes is cell-maturation dependent. J Cell Biochem. 2000;79(1).
97. Muntiu A, Papait A, Vincenzoni F, Vitali A, Lattanzi W, Romele P et al. Disclosing the molecular profile of the human amniotic mesenchymal stromal cell secretome by filter-aided sample preparation proteomic characterization. Stem Cell Res Ther. 2023;14(1).

98. Shin S, Lee J, Kwon Y, Park KS, Jeong JH, Choi SJ et al. Comparative proteomic analysis of the mesenchymal stem cells secretome from adipose, bone marrow, placenta and Wharton's jelly. Int J Mol Sci. 2021;22(2).
99. Bi Y, Qiao X, Liu Q, Song S, Zhu K, Qiu X et al. Systemic proteomics and miRNA profile analysis of exosomes derived from human pluripotent stem cells. Stem Cell Res Ther. 2022;13(1).
100. Phelps J, Sanati-Nezhad A, Ungrin M, Duncan NA, Sen A. Bioprocessing of mesenchymal stem cells and their derivatives: Toward cell-free therapeutics. Vol. 2018, Stem Cells International. 2018.

Publisher's note